

Deformation of a surfactant-covered drop in a linear flow

Petia M. Vlahovska^{a)} and Michael Loewenberg

Department of Chemical Engineering, Yale University, PO Box 208286, New Haven, Connecticut 06520-8286

Jerzy Blawdziewicz

Department of Mechanical Engineering, Yale University, PO Box 208284, New Haven, Connecticut 06520-8284

(Received 28 January 2005; accepted 20 July 2005; published online 21 October 2005)

We study the effect of adsorbed surfactant on drop deformation in linear flows by means of analytical solutions for small perturbations of the drop shape and surfactant distribution, and by numerical simulations for large distortions. We consider a drop with the same viscosity as the suspending fluid. Under these conditions, the problem simplifies because the disturbance flow field results solely from the interfacial stresses that oppose the distortion of shape and surfactant distribution induced by the incident flow. A general form of perturbation analysis valid for any flow is presented. The analysis can be carried out to arbitrary order given its recursive structure; a third-order perturbation solution is explicitly presented. The expansions are compared to results from boundary integral simulations for drops in axisymmetric extensional and simple shear flows. Our results indicate that under weak-flow conditions, deformation is enhanced by the presence of surfactant, but the leading-order perturbation of the drop shape is independent of the (nonzero) surfactant elasticity. In strong flows, drop deformation depends nonmonotonically on surfactant elasticity. The non-Newtonian rheology in a dilute emulsion that results from drop deformation and surfactant redistribution is predicted. Shear thinning is most pronounced for low values of the surfactant elasticity. In the weak-flow limit with finite surfactant elasticity, the emulsion behaves as a suspension of rigid spheres. In strong flows, the stresses can approach the behavior for surfactant-free drops. © 2005 American Institute of Physics. [DOI: 10.1063/1.2112727]

I. INTRODUCTION

Emulsions and polymer blends are liquid-liquid dispersions ubiquitous in the food and petroleum industries. Knowledge of the rheology of these materials is important since flow is involved in their applications and processing.^{1,2} Emulsions exhibit rich rheological behavior that stems from relaxation of the drop microstructure. Surface active agents are often employed to control properties of these materials.³ Predicting emulsion rheology requires understanding of the coupled drop deformation and surfactant dynamics in flow. The problem is challenging because drop shape and surfactant distribution are not given *a priori* but governed by the balance of viscous and interfacial stresses. Adsorbed surfactant reduces the interfacial tension and thus facilitates deformation. Distortion of shape and surfactant distribution is opposed by capillary stresses, due to deviations from spherical shape, and Marangoni stresses (gradients in the interfacial tension along the surface) arising from inhomogeneities in surfactant concentration. The result is an intricate interplay between the evolution of surfactant redistribution, drop deformation, and bulk flows.

Experimental studies^{4–11} show that the presence of surfactant quantitatively and qualitatively modifies drop deformation. Numerical simulations of the dynamics of deformable surfactant-free drops^{12–14} and surfactant-covered

drops^{15–21} have been developed in an attempt to elucidate the role of the surfactant. Analytical solutions, possible in certain limiting cases, are useful for gaining insights into the underlying physics.

The dynamics of a surfactant-free drop has been extensively studied; it is reviewed in Refs. 22 and 23. Small deformation theories^{24–27} predict drop shape when it is close to a sphere, which is the case when interfacial stresses dominate the viscous stresses. Such analyses are complicated because of the nonlinear dependence of curvature on drop deformation. So far only a second-order perturbation solution has been derived by Barthes-Biesel and Acrivos.²⁶

Similar analyses for a surfactant-covered drop are not as well developed. Effects arising solely from surfactant redistribution have been considered in Refs. 28 and 29, where it was shown that emulsions behave as non-Newtonian fluids even in the absence of drop deformation. Only a few analytical studies have been published that include the effects of surfactants as well as drop deformation in linear flows. First-order small deformation theories for a drop with surfactant on the interface have been developed by Flumerfelt³⁰ and Stone and Leal.⁴ However, these linear models do not capture some of the important features of emulsion rheology, such as normal stresses. A higher-order perturbation solution is needed in order to predict the nonlinear deformation of surfactant-covered drops and the non-Newtonian rheology of an emulsion with deformable surfactant-covered drops.

The hydrodynamic problem of a surfactant-covered drop

^{a)}Present address: MPI-Colloids and Interfaces, Theory Group, D-14424 Potsdam, Germany. Electronic mail: petia@aya.yale.edu

subjected to a viscous flow simplifies considerably when the viscosities of the drop and the suspending fluids are equal. In this case, the drop disturbance flow is due solely to the interfacial stresses. The general integral representation for the velocity field^{31,32} reduces to involve only the “single-layer potential” term with known density given by the interfacial stresses. For a drop, interfacial stresses depend on surface tension, interface curvature, and viscoelasticity of the surfactant layer.^{33,34}

In this paper we present a perturbation solution for the deformation of a surfactant-covered drop suspended in an unbounded fluid that is subjected to an arbitrary linear flow. The theory that we develop exploits the simplification in the integral representation of the velocity field for the case where the drop and suspending fluids have equal viscosity. A third-order perturbation solution is explicitly developed.

The paper is organized as follows. Sections II and III present the general formulation of the problem, Sec. IV discusses the method of solution, Sec. V outlines the derivation of the evolution equations for drop shape and surfactant redistribution, Sec. VI describes the boundary integral method (BIM) used for the numerical simulations, and Sec. VII compares the results from our third-order small-deformation theory with boundary integral simulations of the deformation of a surfactant-covered drop in axisymmetric extensional and simple shear flows.

II. DYNAMICS OF A DROP IN STOKES FLOW

We consider a Newtonian drop with radius a and viscosity η , suspended in a Newtonian fluid with the same viscosity. Creeping flow conditions are assumed. A surfactant monolayer with equilibrium concentration Γ_{eq} is present on the drop interface. The corresponding interfacial tension is σ_{eq} .

The surfactant is assumed to be insoluble in the bulk phases; i.e., a fixed mass of surfactant is adsorbed on the drop interface. This assumption holds provided that the time scale for surfactant adsorption/desorption from the bulk phases is long compared to the time scale for surfactant redistribution on the interface. Diffusion of surfactant on the drop interface is usually unimportant²⁹ and is therefore neglected.

A. Incident flow

The drop is placed in a steady two-dimensional linear flow

$$\mathbf{u}^\infty(\mathbf{r}) = \dot{\gamma} \mathbf{E} \cdot \mathbf{r}, \quad (1)$$

where $\dot{\gamma}$ is the strain rate. The general form of the symmetric part \mathbf{E}^s of the velocity gradient \mathbf{E} for a two-dimensional linear flow is

$$\mathbf{E}^s = \sum_{m=-2}^2 \beta_{2m} \mathbf{a}_{2m}, \quad (2)$$

where \mathbf{a}_{2m} is a basis of second-order symmetric traceless spherical tensors defined by Eq. (A17). For example, the axisymmetric extensional flow,

$$\mathbf{u}^\infty = \dot{\gamma} \left(-\frac{1}{2}x, -\frac{1}{2}y, z \right),$$

corresponds to $\beta_{20} = \sqrt{6}/2$ and $\beta_{2m} = 0$ for $m \neq 0$.

B. Dimensionless parameters

The flow distorts the drop shape and redistributes the surfactant. The magnitude of the deformation is characterized by two dimensionless parameters. The capillary parameter (inverse capillary number) is defined by the ratio of shape-preserving surface tension stresses to the shape-distorting viscous stresses induced by the incident flow field

$$\kappa = \frac{\sigma_{\text{eq}}}{\eta a \dot{\gamma}}. \quad (3)$$

Surface tension gradients (Marangoni stresses) tend to maintain a uniform distribution of surfactant on the drop interface. The Marangoni number is the ratio of the Marangoni stresses to the viscous stresses that distort the surfactant distribution

$$\text{Ma} = \frac{\Delta \sigma}{\eta a \dot{\gamma}}, \quad (4)$$

where

$$\Delta \sigma = - \Gamma_{\text{eq}} \left(\frac{\partial \sigma}{\partial \Gamma} \right)_{\Gamma = \Gamma_{\text{eq}}}$$

is the characteristic change of surface tension resulting from perturbations of the local surfactant concentration Γ about the equilibrium value Γ_{eq} .

The ratio of the Marangoni and capillary parameters yields the surfactant elasticity parameter

$$E = \frac{\text{Ma}}{\kappa}, \quad (5)$$

which is a purely physicochemical quantity independent of the flow.⁴ Low-molecular-weight surfactants in emulsions and foams form monolayers with low elasticity $E < 1$ (Ref. 19); high-molecular-weight surfactants such as proteins can form stiffer monolayers.^{35,36}

The drop shape remains approximately spherical provided that the capillary parameter is large, and the surfactant distribution remains nearly uniform if the Marangoni number is large. The two independent parameters used in our analysis are κ and E . Given that $E = O(1)$, it follows that the small deformation analysis presented in this paper is valid for $\kappa^{-1} \ll 1$.

Henceforth, the surfactant concentration is normalized by Γ_{eq} ; all other quantities are rescaled using η , a , and $\dot{\gamma}$. Accordingly, the time scale is $\dot{\gamma}^{-1}$, the velocity scale is $\dot{\gamma} a$, bulk stresses are scaled with $\eta \dot{\gamma}$, and the scale for interfacial tension is σ_{eq} .

C. Interfacial stresses

At rest, the surfactant distribution is uniform on the drop interface and the drop shape is spherical. The difference between the pressure inside and outside the drop is balanced by the interfacial tension,

$$p^{\text{in}} - p^{\text{out}} = 2 \frac{\sigma_{\text{eq}}}{a}. \quad (6)$$

When placed in a flow, the drop produces a disturbance flow field. The latter, given that the drop and the suspending fluids have the same viscosity, arises solely from stresses at the drop interface. The interfacial stress \mathbf{t} can be expressed as the divergence of a surface stress tensor \mathbf{P}

$$\mathbf{t} = -\nabla_s \cdot \mathbf{P}, \quad (7)$$

where

$$\mathbf{P} = \mathbf{I}_s \sigma. \quad (8)$$

The surface gradient operator is defined as

$$\nabla_s = \mathbf{I}_s \cdot \nabla, \quad (9)$$

where $\mathbf{I}_s = \mathbf{I} - \mathbf{n}\mathbf{n}$ is the surface projection, and \mathbf{n} is the unit normal vector to the interface.

For small perturbations from equilibrium, the surfactant equation of state can be linearized. In dimensionless variables, we have

$$\sigma(\Gamma) = 1 - E(\Gamma - 1), \quad (10)$$

where E is the elasticity (5). Combining Eqs. (7)–(10) we obtain the interfacial stress

$$\mathbf{t} = \kappa \mathbf{t}^{\text{cap}} + \text{Ma} \mathbf{t}^{\text{mar}}, \quad (11)$$

where

$$\mathbf{t}^{\text{cap}} = \mathbf{n} \nabla \cdot \mathbf{n}, \quad \mathbf{t}^{\text{mar}} = -\mathbf{n}(\Gamma \nabla \cdot \mathbf{n}) + \nabla_s \Gamma. \quad (12)$$

III. DROP SHAPE EVOLUTION

A. Description of the drop shape

In a coordinate system centered at the drop, the radial position r_s of the drop interface can be represented as

$$r_s = \alpha + \varepsilon f(\Omega), \quad (13)$$

where Ω is the solid angle and f is the deviation of drop shape from sphericity, which depends only on the angle Ω and has a vanishing angular average,

$$\int f \, d\Omega = 0. \quad (14)$$

The isotropic contribution α is determined by the volume-conservation constraint

$$\int (\alpha + \varepsilon f)^3 \, d\Omega = 4\pi, \quad (15)$$

with the integration performed over the unit sphere. The magnitude of the perturbation is scaled by a dimensionless parameter ε , the particular choice of which depends on the nature of the problem under consideration.²² For example, in

weak flows a suitable choice for ε is the inverse capillary parameter, κ^{-1} .

Equation (15) shows that the isotropic contribution α depends on the shape perturbation f , thereby complicating the perturbation computations. To facilitate the perturbation analysis, it is convenient to introduce the following rescaled variables,

$$\tilde{r} = \alpha^{-1} r, \quad \tilde{p} = \alpha p, \quad \tilde{f} = \alpha^{-1} f, \quad (16)$$

and the rescaled dimensionless parameters,

$$\tilde{\kappa} = \alpha^{-2} \kappa, \quad \tilde{\text{Ma}} = \alpha^{-3} \text{Ma}. \quad (17)$$

Since in rescaled variables the radial position of the drop interface is expressed in terms of a deviation from a sphere of unit radius,

$$\tilde{r}_s = 1 + \varepsilon \tilde{f}(\Omega), \quad (18)$$

rather than a sphere of unknown radius α (13), the perturbation analysis is simplified; for small deviations from sphericity, the boundary conditions are linearized and applied at $\tilde{r} = 1$.

Hereafter we omit the tilde for rescaled variables and work only in rescaled variables (unless otherwise indicated). After solving for the drop deformation in rescaled variables we revert to the actual quantities by means of the transformations (16) and (17).

B. Evolution equation for drop shape

The evolution of the interface is governed by³⁷

$$\frac{\partial H}{\partial t} + \mathbf{u}_s \cdot \nabla H = 0, \quad (19)$$

where \mathbf{u}_s is the fluid velocity at the drop interface. The function $H(\mathbf{r}, t)$ represents the interface shape as the set of points \mathbf{r} , where $H(\mathbf{r}, t) \equiv 0$, and is given by the relation

$$H(\mathbf{r}, t) = r - r_s(\Omega, t). \quad (20)$$

In terms of the shape perturbation f the evolution of the interface (19) reads

$$\varepsilon \frac{\partial f}{\partial t} = \mathbf{u}_s \cdot (\hat{\mathbf{r}} - \varepsilon \nabla f), \quad (21)$$

where $\hat{\mathbf{r}} = \mathbf{r}/r$. The outward pointing unit normal to the drop interface is defined in terms of the shape function H as

$$\mathbf{n} = \frac{\nabla H}{|\nabla H|}. \quad (22)$$

After introducing (18) and (20) in the above definition, it becomes

$$\mathbf{n} = (r_s \hat{\mathbf{r}} - \varepsilon \nabla f) [r_s^2 + \varepsilon^2 \nabla f \cdot \nabla f]^{-1/2}. \quad (23)$$

C. Evolution equation for surfactant distribution

Conservation of an insoluble nondiffusing surfactant requires³⁸

$$\frac{d}{dt} \int_{\delta S(t)} \Gamma dA = 0, \quad (24)$$

where $\delta S(t)$ is a material element on the drop interface. By the Reynolds transport theorem for a material surface element, we obtain the conservation equation

$$\frac{\partial \Gamma}{\partial t} + \nabla_s \cdot (\Gamma \mathbf{u}) = 0. \quad (25)$$

The evaluation of the surface divergence term on the deformed interface involves a rather tedious algebra. To circumvent this problem, we introduce the angular surfactant distribution, Γ_Ω , defined as the projection of the surfactant density Γ from the deformed interface onto a sphere,

$$\Gamma = \frac{\Gamma_\Omega}{J(f)}, \quad (26)$$

where $J(f)$ is the Jacobian of the transformation

$$J(f) = \frac{r_s^2}{\hat{\mathbf{r}} \cdot \mathbf{n}}. \quad (27)$$

The surfactant conservation equation in angular variables assumes a simpler form:

$$\frac{\partial \Gamma_\Omega}{\partial t} + \nabla_\Omega \cdot (\Gamma_\Omega \mathbf{u}_\Omega) = 0, \quad (28)$$

where ∇_Ω denotes the angular part of the gradient operator, and \mathbf{u}_Ω is the angular surface velocity, which is tangential to a sphere,

$$\mathbf{u}_\Omega = r_s^{-1} (\mathbf{I} - \hat{\mathbf{r}}\hat{\mathbf{r}}) \cdot \mathbf{u}_s. \quad (29)$$

The flow-induced perturbation in the angular surfactant concentration is

$$\Gamma_\Omega = 1 + \varepsilon g(\Omega), \quad (30)$$

where

$$\int g d\Omega = 0, \quad (31)$$

thus the evolution equation (28) becomes

$$\varepsilon \frac{\partial g}{\partial t} = -\nabla_\Omega \cdot (\mathbf{u}_\Omega) - \varepsilon \nabla_\Omega \cdot (g \mathbf{u}_\Omega). \quad (32)$$

Note that since the angular surfactant concentration (26) is defined on a sphere, conservation of the total surfactant amount is automatically satisfied and complications similar to those encountered with the conservation of drop volume (15) are avoided.

D. Expansion in spherical harmonics

In Eqs. (18) and (30), the functions f and g representing the perturbations of the drop shape and surfactant distribution depend only on angular coordinates. Thus, these functions are expanded into series of scalar spherical harmonics Y_{jm} [see Eq. (A1)]:

$$f = \sum_{j=2}^{\infty} \sum_{m=-j}^j f_{jm} Y_{jm}, \quad (33a)$$

$$g = \sum_{j=2}^{\infty} \sum_{m=-j}^j g_{jm} Y_{jm}. \quad (33b)$$

In the above equations, the summation starts from nonzero j because f and g include only the nonisotropic contributions, according to Eqs. (14) and (31).

The external linear flow (1) is fully characterized by a second-order traceless tensor, which corresponds to spherical harmonics of the order $j=2$. Moreover, the external flow field is invariant with respect to the simultaneous reflection of the axis x and y . These symmetry properties imply that

$$f_{jm} = 0, \quad g_{jm} = 0 \text{ for odd } j \text{ or } m, \quad (34)$$

provided that the drop is initially spherical with a uniform distribution of surfactant.

Starting with Eqs. (21) and (32), our goal is to derive a set of coupled evolution equations

$$\varepsilon \frac{\partial f_{jm}}{\partial t} = F_{jm}(\mathbf{f}, \mathbf{g}), \quad (35)$$

$$\varepsilon \frac{\partial g_{jm}}{\partial t} = G_{jm}(\mathbf{f}, \mathbf{g}) \quad (36)$$

for the shape and surfactant parameters

$$\mathbf{f} \equiv \{f_{jm}\}, \quad \mathbf{g} \equiv \{g_{jm}\}. \quad (37)$$

The equations will be obtained as a power series in the magnitude of the perturbation ε ,

$$F_{jm}(\mathbf{f}, \mathbf{g}) = \sum_{p=0}^{\infty} \varepsilon^p F_{jm}^{(p)}(\mathbf{f}, \mathbf{g}), \quad (38)$$

$$G_{jm}(\mathbf{f}, \mathbf{g}) = \sum_{p=0}^{\infty} \varepsilon^p G_{jm}^{(p)}(\mathbf{f}, \mathbf{g}). \quad (39)$$

The derivation of the above equations requires computation of the interfacial velocity field \mathbf{u}_s and transformation of the quantities on the right-hand sides of Eqs. (21) and (32) into the spherical-harmonics representation.

IV. MULTIPOLE REPRESENTATION OF INTERFACIAL VELOCITY

In this paper we focus on the dynamics of drop with the same viscosity as the continuous-phase fluid. Therefore the fluid velocity field \mathbf{u} satisfies the Stokes equations

$$\nabla^2 \mathbf{u} - \nabla p = -\mathbf{F}(\mathbf{r}), \quad \nabla \cdot \mathbf{u} = 0, \quad (40)$$

in the whole space, where

$$\mathbf{F}(\mathbf{r}) = \mathbf{t}(\mathbf{r}_s) \delta_s(\mathbf{r}) \quad (41)$$

is the surface force density associated with the interfacial stress given by Eqs. (11) and (12), and

$$\delta_s(\mathbf{r}) = \int_S \delta(\mathbf{r} - \mathbf{r}_s) d^2\mathbf{r}_s. \quad (42)$$

At infinity, the flow field \mathbf{u} tends to the incident flow $\mathbf{u} \rightarrow \mathbf{u}^\infty$.

Unlike the case of drops with viscosity contrast, in the present case the solution of Eq. (40) for the disturbance field

$$\bar{\mathbf{u}}(\mathbf{r}) = \mathbf{u}(\mathbf{r}) - \mathbf{u}^\infty(\mathbf{r}) \quad (43)$$

can be evaluated directly from the force distribution (41)

$$\bar{\mathbf{u}}(\mathbf{r}) = \int_S \mathbf{T}(\mathbf{r} - \mathbf{r}') \cdot \mathbf{F}(\mathbf{r}') d\mathbf{r}', \quad (44)$$

where

$$\mathbf{T}(\mathbf{r}) = \frac{1}{8\pi r} (\mathbf{I} + \hat{\mathbf{r}}\hat{\mathbf{r}}) \quad (45)$$

is the Oseen tensor.³¹ Thus, the complications posed by the usual approach of solving Stokes equations separately for the regions inside and outside the drop and matching the solutions on the deformed drop interface^{22,26} are avoided.

In the present study we find the disturbance flow field (44) by using a multipole expansion method. Accordingly, the force distribution is represented as a collection of force multipoles; the strengths of the multipoles are obtained as the moments of the surface force distribution (41). The disturbance field $\bar{\mathbf{u}}$ is then represented as the superposition of the corresponding multipolar velocity fields. This procedure is analogous to the multipolar expansion method in electrostatics.³⁹

In our approach we use the multipole representation of the Stokes flow introduced by Cichocki *et al.*⁴⁰ In this representation the strengths of the force multipoles c_{jmq} are given by

$$c_{jmq} = - \int_S \mathbf{v}_{jmq}^+(\mathbf{r}) \cdot \mathbf{F}(\mathbf{r}) d\mathbf{r}. \quad (46)$$

The corresponding expansion of the disturbance velocity field outside the drop is

$$\bar{\mathbf{u}}^{\text{out}}(\mathbf{r}) = \sum_{jmq} c_{jmq} \mathbf{v}_{jmq}^-(\mathbf{r}). \quad (47)$$

The functions \mathbf{v}_{jmq}^\pm form basis sets of fundamental solutions of the Stokes equations,⁴⁰ and have a separable form

$$\mathbf{v}_{jmq}^+(\mathbf{r}) = \mathbf{V}_{jmq}^+(\Omega) r^{j+q-1}, \quad (48)$$

$$\mathbf{v}_{jmq}^-(\mathbf{r}) = \mathbf{V}_{jmq}^-(\Omega) r^{-(j+q)}. \quad (49)$$

The functions \mathbf{V}_{jmq}^\pm are combinations of vector spherical harmonics with angular and azimuthal quantum numbers j and m ; the explicit definitions are listed in Appendix E.

The evolution equations (21) and (32) involve the velocity field at the drop interface, which using relations (43), (47), and (49) is

$$\mathbf{u}_s = \mathbf{u}_s^\infty + \sum_{jmq} c_{jmq} r_s^{-(j+q)} \mathbf{V}_{jmq}^-(\Omega), \quad (50)$$

where

$$\mathbf{u}_s^\infty = r_s \mathbf{E} \cdot \hat{\mathbf{r}} \quad (51)$$

is the imposed velocity field (1) evaluated at the drop interface $r=r_s$. The expansion coefficients c_{jmq} in the above equation are obtained by inserting Eq. (41) into (46), and using relation (48),

$$c_{jmq} = - \int r_s^{j+q-1} \mathbf{V}_{jmq}^+ \cdot \mathbf{t}(\mathbf{f}, \mathbf{g}) J(\mathbf{f}) d\Omega, \quad (52)$$

where $J(\mathbf{f})$ is the Jacobian defined by Eq. (27). Relations (47) and (52) constitute the solution for the velocity fields. In the following section, Eqs. (50) and (52) are used to obtain the evolution equations for the drop shape and the surfactant distributions.

V. SOLUTION OUTLINE

The underlying structure of the perturbation expansions (38) and (39) for the evolution of drop shape and surfactant distribution, as well as velocity and stress fields, consists of a “double” expansion: (i) in spherical harmonics (33a), (33b), and (47), and (ii) in the small parameter ε , which measures the magnitude of the deformation.

For small deviation from sphericity, $\varepsilon \ll 1$, the exact position of the interface at $r=1+\varepsilon f$ is replaced by the equilibrium position, $r=1$, and all quantities that are to be evaluated at the interface of the deformed drop are approximated using a Taylor series expansion.

The derivation of the shape and surfactant evolution equations (38) and (39) involves two steps. In the first step, the expansions for surface velocity (50), angular velocity (29) as well as geometric quantities such as gradient of shape perturbation, ∇f , are obtained. In the second step, these expansions are inserted in the evolution equations (21) and (32) and the products of spherical harmonics are manipulated to yield the final form of the evolution equations (35) and (36).

This solution procedure is outlined below. The detailed calculations, which require tedious algebra, were performed using MATHEMATICA. More information is given in the Appendices and in Ref. 41.

A. Expansion for the velocity field

The velocity coefficients (52) are obtained as perturbation expansion in the small parameter ε ,

$$c_{jmq} = \sum_{p=0}^{\infty} \varepsilon^p c_{jmq}^{(p)}(\mathbf{f}, \mathbf{g}). \quad (53)$$

The derivation involves expanding around the spherical drop shape position of the deformed interface r_s (18), the interfacial stresses $\mathbf{t}(\mathbf{f}, \mathbf{g})$ (11) and (12), and the Jacobian $J(\mathbf{f})$ (27).

The expansion procedure is explained on the example of the interfacial stresses:

$$\mathbf{t} = \sum_{p=0}^{\infty} \varepsilon^p \mathbf{t}^{(p)}(\mathbf{f}, \mathbf{g}). \quad (54)$$

The expansion coefficients $\mathbf{t}^{(p)}$ are homogeneous functions of order p jointly in f, g , i.e., involving combinations of f and g in the form

$$\mathbf{t}^{(p)} \sim f^n g^{p-n}, \quad n = 0, \dots, p. \quad (55)$$

Therefore, after inserting the spherical harmonics representation of f and g (33a) and (33b), an expansion term of order p contains products of p harmonics.

In our approach the products of spherical harmonics are transformed into a sum of harmonics. A well-developed theory exists for this procedure.^{42,43} Here we summarize the general ideas; the explicit recoupling formulas are listed in Appendix A 2.

The recoupling expression for scalar harmonics has the form⁴⁴

$$Y_{j'm'} Y_{j''m''} = \sum_{\mathbf{j}\mathbf{m}} \zeta(\mathbf{j}, \mathbf{m}) Y_{\mathbf{j}\mathbf{m}}. \quad (56a)$$

Here

$$\mathbf{j} \equiv \{j, j', j''\}, \quad \mathbf{m} \equiv \{m, m', m''\}$$

denote the set of angular and azimuthal numbers, and $\zeta(\mathbf{j}, \mathbf{m})$ are the Clebsch-Gordan coefficients,⁴⁴ given by Eq. (A11). Simple algorithms are readily available for the computations of these coefficients.⁴² For products involving vector spherical harmonics the structure of the recoupling expressions is similar:

$$\mathbf{y}_{j'm'q'} Y_{j''m''} = \sum_{\mathbf{j}\mathbf{m}} C_1(\mathbf{j}) \zeta(\mathbf{j}, \mathbf{m}) \mathbf{y}_{\mathbf{j}\mathbf{m}}, \quad (56b)$$

$$\mathbf{y}_{j'm'q'} \cdot \mathbf{y}_{j''m''q''} = \sum_{\mathbf{j}\mathbf{m}} C_2(\mathbf{j}) \zeta(\mathbf{j}, \mathbf{m}) Y_{\mathbf{j}\mathbf{m}}, \quad (56c)$$

with the same dependence on the azimuthal numbers \mathbf{m} , but different dependence on the angular numbers \mathbf{j} , represented by the factors C_1 and C_2 . Explicit expressions for these coefficients are given by (A6) and (A8). Products of three and more harmonics are recoupled by iterative evaluation of the nested products of two harmonics as outlined in Appendix B 4. For example,

$$Y_{j_1 m_1} Y_{j_2 m_2} Y_{j_3 m_3} = \left(\sum \zeta(\mathbf{j}, \mathbf{m}) Y_{\mathbf{j}\mathbf{m}} \right) Y_{j_3 m_3}, \quad (57)$$

and then the product of each of the terms in the sum, $Y_{\mathbf{j}\mathbf{m}}$, with $Y_{j_3 m_3}$, is recoupled.

Performing the recoupling procedure in (54), results in the following expansion for interfacial stresses:

$$\mathbf{t} = \sum_{p, \mathbf{j}\mathbf{m}q} \varepsilon^p t_{\mathbf{j}\mathbf{m}q}^{(p)}. \quad (58)$$

Explicit expressions for the first three expansion terms $t_{\mathbf{j}\mathbf{m}q}^{(p)}$, $p=0,1,2$, are listed in Appendix C. By a similar procedure, expansions are derived for the Jacobian and the powers of r_s ,

$$J = \sum_{p, \mathbf{j}\mathbf{m}} \varepsilon^p J_{\mathbf{j}\mathbf{m}}^{(p)} Y_{\mathbf{j}\mathbf{m}}, \quad r_s^k = \sum_{p, \mathbf{j}\mathbf{m}} \varepsilon^p R_{\mathbf{j}\mathbf{m}}^{(p)} Y_{\mathbf{j}\mathbf{m}}. \quad (59)$$

Combining the three expansions (58) and (59) in (52), followed by collecting terms of the same power in ε , recoupling the products of harmonics according to (56a)–(56c), and using the relation

$$\int Y_{\mathbf{j}\mathbf{m}} d\Omega = \sqrt{4\pi} \delta_{j0} \delta_{m0}, \quad (60)$$

yields the expansion coefficients in (53). Explicit expressions for the first three terms $c_{\mathbf{j}\mathbf{m}q}^{(p)}$, obtained using MATHEMATICA, are listed in Appendix E.

B. Expansion of the evolution equations

To obtain the expansion (35) of the drop shape evolution equation (21), we combined the Taylor expansion (around the undeformed, spherical shape) of the surface velocity (50) and the gradient of shape perturbation expansion (B12). Thereafter, we recoupled the scalar product of vector harmonics according to (A8). This procedure yields for the expansion terms (38)

$$F_{\mathbf{j}\mathbf{m}}^{(p)}(\mathbf{f}, \mathbf{g}) = S_{\mathbf{j}\mathbf{m}}^{F, (p)}(\mathbf{f}) + \kappa K_{\mathbf{j}\mathbf{m}}^{F, (p)}(\mathbf{f}^p) + \text{Ma} M_{\mathbf{j}\mathbf{m}}^{F, (p)}(\mathbf{f}^n \mathbf{g}^{p-n}), \quad (61)$$

where n takes values between 0 and p (55).

In a similar fashion, the expansion form (39) of the surfactant evolution equation (32) is derived,

$$G_{\mathbf{j}\mathbf{m}}^{(p)}(\mathbf{f}, \mathbf{g}) = S_{\mathbf{j}\mathbf{m}}^{\Gamma, (p)}(\mathbf{f}^n \mathbf{g}^{p-n}) + \kappa K_{\mathbf{j}\mathbf{m}}^{\Gamma, (p)}(\mathbf{f}^n \mathbf{g}^{p-n}) + \text{Ma} M_{\mathbf{j}\mathbf{m}}^{\Gamma, (p)}(\mathbf{f}^n \mathbf{g}^{p-n}). \quad (62)$$

In the above equations, the terms $S_{\mathbf{j}\mathbf{m}}^{(p)}$ describe the effects of the imposed flow on the shape and surfactant distribution. Since the drop and suspending fluids have no viscosity contrast, in linear flows (51)

$$S_{\mathbf{j}\mathbf{m}}^{(p)} = 0 \quad \text{for } p > 1. \quad (63)$$

The terms $K_{\mathbf{j}\mathbf{m}}^{(p)}$, which are proportional to the capillary parameter (3), describe relaxation driven by capillary stresses (11). The terms $M_{\mathbf{j}\mathbf{m}}^{(p)}$, which multiply the Marangoni number (4), describe the Marangoni stress-driven dynamics.

The capillary and Marangoni terms, $C_{\mathbf{j}\mathbf{m}}^{(p)} = K_{\mathbf{j}\mathbf{m}}^{(p)}, M_{\mathbf{j}\mathbf{m}}^{(p)}$, are a combination of terms with general structure

$$C_{\mathbf{j}\mathbf{m}}^{(p)} \sim \zeta^{p-1}(\mathbf{j}, \mathbf{m}) \mathcal{B}_{np}(\mathbf{j}) \mathbf{f}^n \mathbf{g}^{p-n}, \quad (64)$$

i.e., the p th-order term in the perturbation expansions (61) and (62) involves products of p shape and surfactant parameters, $p-1$ Clebsch-Gordan coefficients, denoted by $\zeta^{p-1}(\mathbf{j}, \mathbf{m})$ (A11), and a term $\mathcal{B}_{np}(\mathbf{j})$, which is an algebraic function of angular numbers \mathbf{j} . The $\zeta^{p-1}(\mathbf{j}, \mathbf{m})$ coefficients arise from recoupling the product of p spherical harmonics using (56a)–(56c). The coefficients $\mathcal{B}_{np}(\mathbf{j})$ are independent of the azimuthal numbers \mathbf{m} and therefore of the type of imposed flow. The universality of the $\mathcal{B}_{np}(\mathbf{j})$ term greatly reduces the amount of information needed to find the solution for a particular imposed linear flow—once derived, the coefficients $\mathcal{B}_{np}(\mathbf{j})$ apply to any type of imposed flow (2).

We have evaluated the coefficients S, K, M up to the third order $p=3$ in the shape perturbation parameter ε and arbitrary spherical-harmonics order j . Explicit expressions of the evolution coefficients for $p=0,1,2$ are listed in Appendix D. The third-order expressions $p=3$ are very cumbersome and can be found in Vlahovska.⁴¹

Previous works on surfactant-free drops by Barthès-Biesel and Acrivos^{26,45} employed tensorial representation for drop deformation, velocity, and stress fields. Manipulating tensors involves tedious algebra, which was performed only for tensors of rank $j=2$ and 4; sixth-order tensors were neglected. As a result, their analysis is incomplete at $O(\varepsilon^2)$, as noted by Rallison.²⁷ However, this does not affect their solution for the case $\lambda=1$ considered herein.

In the present work, we overcome these limitations by taking advantage of the well-developed formalism for manipulation of spherical harmonics and by employing the multipole representation of the velocity. This makes it possible to carry out the double expansion, in spherical harmonics and in the small shape perturbations, to arbitrary high orders. The relation between the spherical harmonics and tensorial notations can be found in Vlahovska.⁴¹

C. Emulsion rheology

The effective stress of a dilute emulsion with drop volume fraction ϕ is

$$\Sigma = 2\mathbf{E} + \phi\mathbf{T}^d, \quad (65)$$

where the drop contribution is given in a form of the perturbation expansion

$$\mathbf{T}^d = \sum \varepsilon^p \mathbf{T}^{(p)}. \quad (66)$$

Rheological properties of interest are the shear stress, T_{12}^d , and the normal stress differences, $N_1 = T_{11}^d - T_{22}^d$, $N_2 = T_{22}^d - T_{33}^d$. Drop stress is directly related to the force multipoles, given by Eq. (46).²⁸ Inserting the expansion (53) leads to

$$T_{12}^{(p)} = -\frac{i}{8} \sqrt{\frac{6}{5\pi}} (c_{220}^{(p)} - c_{2-20}^{(p)}), \quad (67a)$$

$$N_1^{(p)} = \frac{1}{4} \sqrt{\frac{6}{5\pi}} (c_{220}^{(p)} + c_{2-20}^{(p)}), \quad (67b)$$

$$N_2^{(p)} = -\frac{1}{2} N_1^{(p)} + \frac{3}{4} \sqrt{\frac{1}{5\pi}} c_{200}^{(p)}. \quad (67c)$$

VI. BOUNDARY INTEGRAL SIMULATIONS

Boundary integral simulations of the drop dynamics were constructed by representing the drop interface and surfactant distribution on a triangular mesh with nodes \mathbf{x}_i ($i=1, \dots, N$), which have corresponding area weights w_i . An adaptive discretization algorithm was used to maintain resolution of the evolving drop shape and surfactant distribution.⁴⁶

The evolution of the interface shape and surfactant distribution was obtained by integrating the kinematic relation

$$\frac{d\mathbf{x}_i}{dt} = \mathbf{u}_i, \quad (68)$$

and the discretized conservation constraint (24)

$$\frac{d}{dt}(\Gamma_i w_i) = 0. \quad (69)$$

Here \mathbf{u}_i is the fluid velocity and Γ_i is the surfactant concentration at a node \mathbf{x}_i .

The fluid velocities \mathbf{u}_i ($i=1, \dots, N$) were obtained from Eq. (44) by numerical quadrature using cylindrical coordinates to remove the r^{-1} singularity of the Oseen tensor (45). The surface force density (41) was computed by differentiating quadratic approximations⁴⁷ of the local drop shape and surfactant distribution as needed to evaluate the local normal vector, mean curvature, and the surfactant concentration gradient.

VII. RESULTS

In this section we present results for drop deformation in some common types of linear flows: axisymmetric extensional, simple shear, and hyperbolic flows. We focus our attention on steady-state drop deformation; however, our analysis can also be used to explore transient flows.

We have evaluated the expansion terms in the shape and evolution equations (61) and (62) for perturbation order $p \leq 3$. The perturbation coefficients for a surfactant-free drop agree with the ones derived by Barthès-Biesel.²⁶

The accuracy of the expansion (61) and (62) depends on two factors: the number perturbation terms and the number of spherical harmonics in the basis describing the shape and surfactant distribution (33a) and (33b). In our calculations we obtained numerical convergence by expanding up to perturbation order $p=3$ and spherical harmonic order $j \leq 4$. However, in the interim calculations at perturbation order p harmonics of up to order $4p+2$ must be retained in the description of the velocity and stress fields.

We present theoretical calculations for drop deformation and the effective stress of an emulsion consisting of deformable surfactant-covered drops in the weak-flow limit, where the small parameter is the flow strength $\varepsilon \equiv \kappa^{-1}$. The predictions from the small-deformation theory are compared to numerical boundary-integral simulations.

A. Weak-flow expansions

In this section we provide explicit expressions for the expansions of shape, surfactant concentration, and stresses in the case of simple shear flow. The shape and surfactant parameters (33a) and (33b) are decomposed into real and imaginary parts:

$$f_{j\pm m} = f'_{jm} \pm i f''_{jm} \quad \text{and} \quad g_{j\pm m} = g'_{jm} \pm i g''_{jm}. \quad (70)$$

For $m=0$, the shape and surfactant parameters are real. Deformations of $2z^2 - x^2 - y^2$, $x^2 - y^2$, and xy types are characterized by f'_{20} , f'_{22} , and f''_{22} .

1. Surfactant-free drop

Here we recover the previously derived second-order shape and stress expansions of Barthes-Biesel and Acrivos,^{26,45} and extend their results to third order.

To third order, the expansion for the steady-state drop shape deformation can be written as

$$f_{jm} = f_{1,jm}\kappa^{-1} + f_{2,jm}\kappa^{-2} + f_{3,jm}\kappa^{-3}. \quad (71)$$

At leading order the only nonzero contribution is

$$f''_{1,22} = -\frac{7}{8}\sqrt{\frac{5\pi}{6}}. \quad (72)$$

At the next order, the nonzero contributions are

$$\begin{aligned} f_{2,20} &= -\frac{1755}{384}\sqrt{5\pi}, & f'_{2,22} &= \frac{245}{128}\sqrt{\frac{5\pi}{6}}, \\ f_{2,40} &= -\frac{469}{3456}\sqrt{\pi}, & f'_{2,44} &= -\frac{469}{3456}\sqrt{\frac{35\pi}{2}}. \end{aligned} \quad (73)$$

At order 3, the nonzero contributions are

$$\begin{aligned} f''_{3,22} &= \frac{343}{512}\sqrt{\frac{15\pi}{2}}, \\ f''_{3,42} &= \frac{767291}{1\,824\,768}\sqrt{\frac{5\pi}{2}}, & f''_{3,44} &= -\frac{18\,179}{6144}\sqrt{\frac{7\pi}{10}}, \\ f''_{3,62} &= -\frac{17\,969}{270\,336}\sqrt{\frac{35\pi}{39}}, & f''_{3,66} &= -\frac{89\,845}{24\,576}\sqrt{\frac{7\pi}{429}}. \end{aligned} \quad (74)$$

The imaginary parts of the shape parameters have expansions in odd powers of κ^{-1} , whereas the real parts have expansions in even powers of κ^{-1} . Correspondingly, the shear stress, which is related to the imaginary parts of the shape parameters, has an expansion in even powers of κ^{-1} , and the normal stresses, which are related to the real part of the shape parameters, have expansions in odd powers of κ^{-1} :

$$\begin{aligned} T_{12} &= \frac{7}{4} - \frac{2107}{512}\kappa^{-2}, \\ N_1 &= \frac{245}{32}\kappa^{-1} - \frac{249\,361}{442\,368}\kappa^{-3}, \\ N_2 &= -\frac{35}{16}\kappa^{-1} - \frac{19\,440\,211}{14\,598\,144}\kappa^{-3}. \end{aligned} \quad (75)$$

At leading order the drop is spherical and the effective viscosity is given by Taylor's result.⁴⁸ Drop deformation gives rise to shear thinning of $O(\kappa^{-2})$ and normal stresses of $O(\kappa^{-1})$.

2. Surfactant-covered drop

To third order in κ^{-1} , the steady-state shape and surfactant distribution are described by the expansions

$$\begin{aligned} f_{jm} &= f_{1,jm}(E)\kappa^{-1} + f_{2,jm}(E)\kappa^{-2} + f_{3,jm}(E)\kappa^{-3}, \\ g_{jm} &= g_{1,jm}(E)\kappa^{-1} + g_{2,jm}(E)\kappa^{-2} + g_{3,jm}(E)\kappa^{-3}. \end{aligned} \quad (76)$$

The convergence radius for these expansions is largest for $E \approx 1$ because the perturbations of the drop shape and surfactant distribution have comparable magnitudes.

Here we list only deformation parameters with $j \leq 4$. At leading order, the only nonzero contributions are

$$f''_{1,22} = -\sqrt{\frac{5\pi}{6}}, \quad g''_{1,22} = -\frac{1+2E}{E}\sqrt{\frac{5\pi}{6}}. \quad (77)$$

At second order, the nonzero contributions are

$$\begin{aligned} f_{2,20} &= -\frac{5}{7}\sqrt{5\pi}, & f'_{2,22} &= \frac{5}{42}\frac{1+11E}{E}\sqrt{\frac{5\pi}{6}}, \\ f_{2,40} &= \frac{5}{28}\sqrt{\pi}, & f'_{2,44} &= -\frac{5}{4}\sqrt{\frac{5\pi}{14}}, \end{aligned} \quad (78)$$

and

$$\begin{aligned} g_{2,20} &= -\frac{5}{42}\frac{5+17E}{E}\sqrt{5\pi}, \\ g'_{2,22} &= \frac{5}{12}\frac{4+8E+11E^2}{E^2}\sqrt{\frac{5\pi}{6}}, \\ g_{2,40} &= \frac{5}{84}\frac{9+4E}{E}\sqrt{\pi}, & g'_{2,44} &= -\frac{5}{12}\frac{9+4E}{E}\sqrt{\frac{5\pi}{14}}. \end{aligned} \quad (79)$$

At third order, the nonzero contributions are

$$\begin{aligned} f''_{3,22} &= \frac{5}{28\,224}\frac{1960+3675E+8909E^2+4704E^3}{E^2}\sqrt{\frac{5\pi}{6}}, \\ f''_{3,42} &= \frac{425}{539}\sqrt{\frac{5\pi}{2}}, \\ f''_{3,44} &= \frac{30-457E-4937E^2}{864E^2}\sqrt{\frac{5\pi}{14}}, \end{aligned} \quad (80)$$

and

$$\begin{aligned} g''_{3,22} &= \frac{5}{14\,112} \\ &\quad \times \frac{7840+6370E+4289E^2-6787E^3+4704E^4}{E^3}\sqrt{\frac{5\pi}{6}}, \\ g''_{3,42} &= \frac{25}{3234}\frac{278+213E}{E}\sqrt{\frac{5\pi}{2}}, \\ g''_{3,44} &= \frac{1080-5847E-10\,691E^2-6574E^3}{864E^3}\sqrt{\frac{5\pi}{14}}. \end{aligned} \quad (81)$$

Additionally, there are two shape and two surfactant parameters associated with the $j=6$ harmonics, however, we obtained numerical convergence with $j \leq 4$ as discussed above.

The expansions for the steady-state stresses are

$$\begin{aligned}
 T_{12} &= \frac{5}{2} - \frac{25}{1176} \frac{98 + 98E + 239E^2}{E^2} \kappa^{-2}, \\
 N_1 &= \frac{5}{2} \frac{4E + 1}{E} \kappa^{-1} - \frac{5}{7056} \frac{2940 + 5789E + 8103E^2 + 7114E^3}{E^2} \kappa^{-3}, \\
 N_2 &= -\frac{5}{28} \frac{13E + 7}{E} \kappa^{-1} + \frac{5}{8\,692\,992} \frac{8\,602\,440 + 2\,124\,199E - 3\,147\,942E^2 + 8\,390\,519E^3 + 2\,587\,200E^4}{E^2} \kappa^{-3}.
 \end{aligned} \tag{82}$$

The limit $\kappa^{-1} \rightarrow 0$ (spherical drops), with nonzero elasticity, corresponds to $\text{Ma}^{-1} \rightarrow 0$. Under these conditions, the surfactant distribution is uniform and the drop interface is tangentially immobile. It follows that the rheology is the same as that for a suspension of rigid spheres.

The regime $E \rightarrow 0$, corresponding to drops with clean interfaces, cannot be recovered from our perturbation solution (76) and (82) because it is a singular limit of our small perturbation expansion; i.e., $E \rightarrow 0$ implies $\text{Ma}^{-1} \rightarrow \infty$ and thus large distortion of the surfactant distribution.

B. Discussion

Drop deformation in an axisymmetric extensional flow and a simple shear flow is illustrated in Figs. 1 and 2. Our results show that drop deformation is insensitive to the surfactant elasticity under weak-flow conditions, in agreement with experiments.¹⁰ This observation is consistent with our perturbation solution which indicates that the leading-order shape deformation is independent of the surfactant elasticity, as seen in the shape expansion for a drop in shear flow equations (76)–(78). In axisymmetric strain, shape deformation in

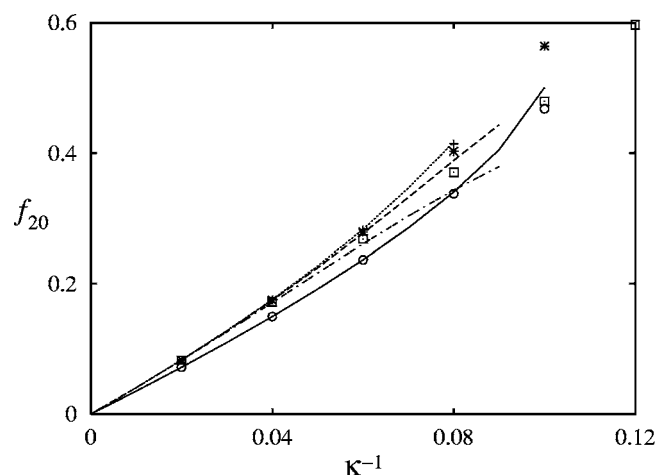


FIG. 1. Drop deformation in axisymmetric straining flow; The shape parameter f_{20} as a function of flow strength κ^{-1} for surfactant-free drop (circles, solid line), $E=0.25$ (crosses, dotted line), $E=1$ (stars, dashed line), $E=4$ (squares, dot-dashed line). The symbols are data from the boundary integral method (BIM) used for numerical simulations. The lines represent the third-order small deformation theory.

stronger flows is suppressed with increased elasticity, as found by Eggleton *et al.*¹⁹ No such conclusion can be drawn for drops in strong shear flows.

Drop deformation and surfactant redistribution each contribute to the shear thinning viscosity and nonzero normal stresses that are generally observed in emulsions. Unlike perturbations of drop shape, perturbations of the surfactant distribution and therefore the emulsion rheology depend on the elasticity at leading order in the capillary parameter.

The drop contributions to the shear viscosity and normal stresses predicted by our small-deformation theory for a dilute emulsion of surfactant-covered deformable drops are compared to our boundary integral simulations in Figs. 3 and 4. The results demonstrate that under weak-flow conditions, our third-order theory quantitatively predicts the shear-thinning viscosity and normal stresses. By contrast, the linear theory⁴ does not predict any of these rheological features.

Figure 3 shows the shear viscosity for drops with surfactant monolayers of different elasticities. At low flow strengths, surfactant immobilizes the interface so that the emulsion behaves as a suspension of rigid spheres. Shear thinning is most pronounced for low values of the surfactant elasticity. For the lowest value of elasticity shown in Fig. 3 ($E=0.25$), the shear viscosity tends to the behavior for surfactant-free drops at sufficiently high shear rates. Under these conditions, the surfactant is passively convected on the drop surface. For larger values of the elasticity, the high-shear-rate regime is inaccessible because of drop breakup.

Normal stresses are shown in Fig. 4. As is usually observed, $N_1 > 0$ and $N_2 < 0$. The $O(\kappa^{-3})$ expansions (82) provide more accurate predictions for the normal stresses than for the shear stress, which explains the closer agreement between the analytical and numerical results seen in Fig. 4.

Our third-order solution gives a slightly better prediction of drop deformation than the incomplete solution of Barthes-Biesel²⁶ for drops with clean interfaces, as illustrated in Fig. 5. The comparison of the linear, quadratic, and cubic expansions shows that the convergence radius is about $\kappa^{-1} \leq 0.06$. The theoretical calculations agree well with the experimental data,⁴⁹ even though the experimental systems have a viscosity ratio $\lambda=1.35$ and $\lambda=0.7$ and our theory is for $\lambda=1$ (insensitivity of drop deformation to viscosity con-

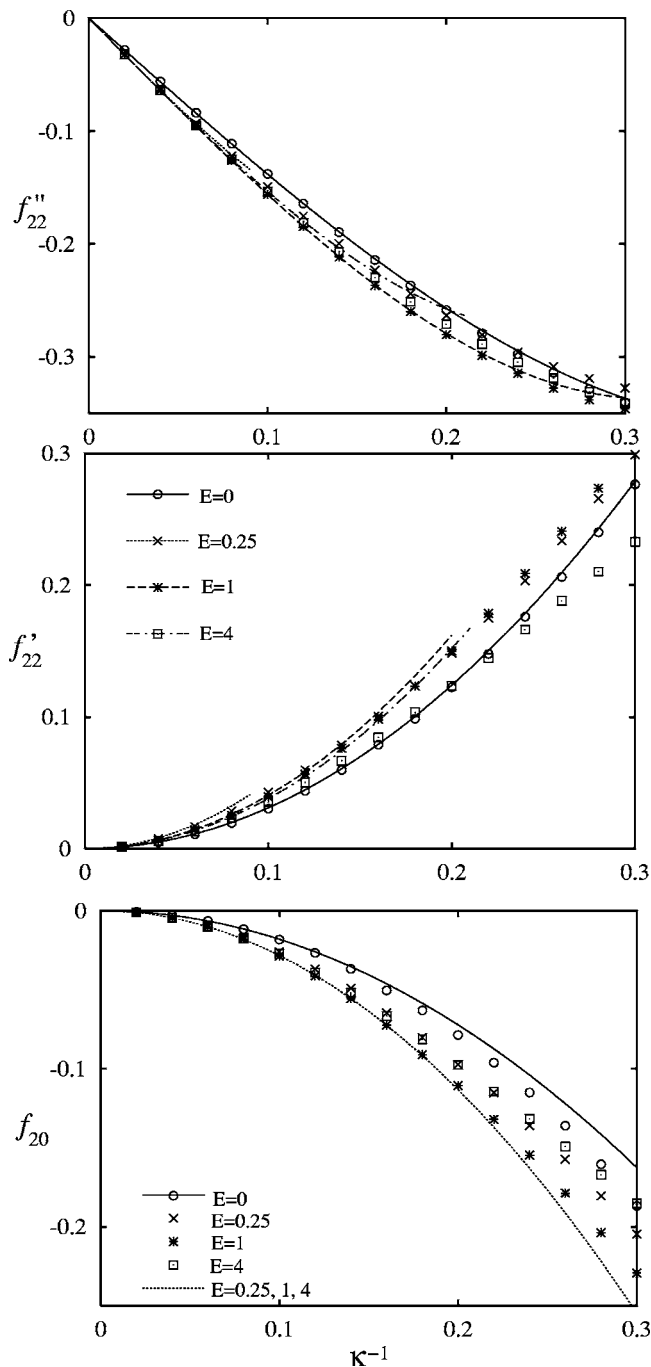


FIG. 2. Drop deformation in a simple shear flow: The shape parameters f''_{22} , f'_{22} and f_{20} as a function of flow strength κ^{-1} for surfactant-free drop (circles, solid line), $E=0.25$ (crosses, dotted line), $E=1$ (stars, dashed line), $E=4$ (squares, dot-dashed line). The points are data from BIM numerical simulation. The lines represent the third-order small deformation theory (76).

trast under weak-flow conditions is consistent with experiments^{50,51} and is predicted by small-deformation theory⁴⁸).

VIII. CONCLUSIONS

A perturbation solution of order $O(\varepsilon^2, \varepsilon^3\kappa, \varepsilon^3\text{Ma})$, where ε measures the magnitude of the shape distortion, was derived to describe the deformation of a surfactant-covered

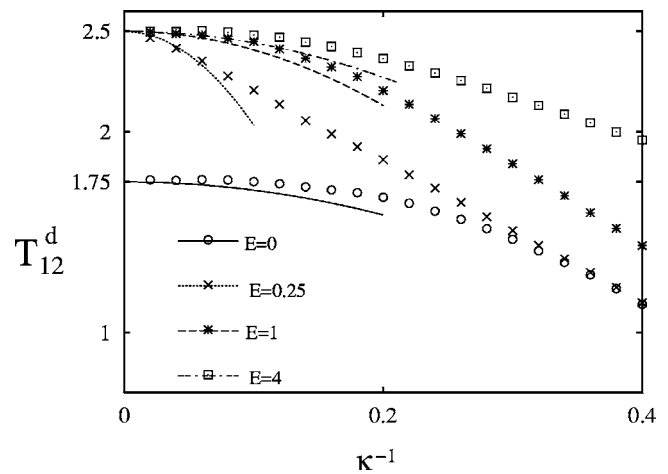


FIG. 3. Dependence of the shear viscosity of an emulsion of surfactant-covered drops on flow strength κ^{-1} at different elasticities of the surfactant monolayer: surfactant-free drop (circles, solid line), $E=0.25$ (crosses, dotted line), $E=1$ (stars, dashed line), $E=4$ (squares, dot-dashed line). The points are data from BIM numerical simulation. The lines represent the third-order small deformation theory (82).

drop in linear viscous flows. Expressions for the shape and surfactant evolution equations, as well as stress and velocity fields, were developed. The solution is applicable for any linear flow under transient or steady-state conditions. Predictions of drop shape, surfactant distribution, and emulsion rheology based on our small-deformation theory are in quan-

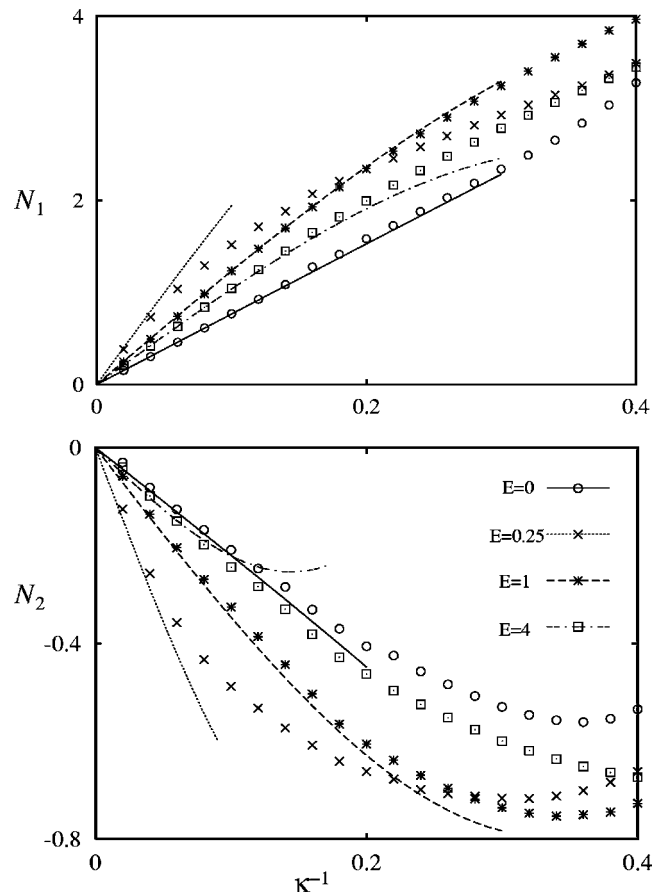


FIG. 4. Same as Fig. 3 but for the normal stress differences.

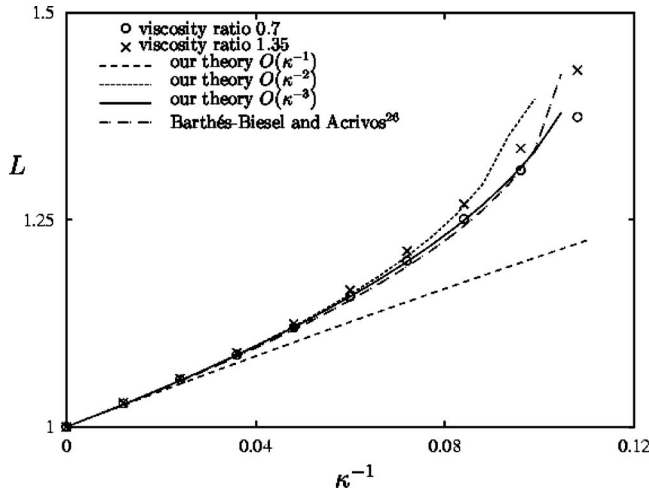


FIG. 5. Surfactant-free drop in a planar hyperbolic flow: Comparison of our small deformation theory and Barthes-Biesel and Acrivos result with experimental data (Ref. 5) for steady-state drop length for drops with viscosity ratios close to 1.

titative agreement with our numerical simulations and in close agreement to experimental data. The perturbation scheme presented herein can in principle be extended to arbitrary order because of its recursive structure.

The problem analyzed in this paper was considerably simplified by assuming that the viscosities of drop and suspending phases are equal. Thus the disturbance velocity field was computed directly from the interfacial stresses using the integral representation of the Stokes flow solution thereby avoiding the evaluation of boundary conditions, e.g., matching inner and outer velocities, on the deformed interface. The analysis was further simplified by rescaling the position of the deformed interface to avoid computational difficulties associated with drop volume conservation. The use of spherical harmonics provided a straightforward way to derive a general solution of the hydrodynamic problem for any linear flow.

An extension of our analysis can be applied to study flow effects on cell dynamics, which are important for many biological phenomena.⁵² A vesicle is a fluid-filled lipid membrane that provides a simple model of a cell. Typically the enclosed and suspending fluid are the same, thus the formulation presented in this paper, together with the appropriate expression for the membrane stresses,^{53,54} can be used to explore vesicle hydrodynamics beyond the linear regime that has been studied so far.⁵⁵⁻⁵⁷

In a forthcoming paper, we consider the dynamics of deformable surfactant-covered drops for systems with viscosity contrast.

APPENDIX A: SPHERICAL HARMONICS

1. Definitions of scalar and vector harmonics

For the sake of completeness, we list the definitions of scalar and vector spherical harmonics.^{42,43} The normalized spherical scalar harmonics are defined as

$$Y_{jm}(\Omega) = \left[\frac{2j+1}{4\pi} \frac{(j-m)!}{(j+m)!} \right] (-1)^m P_j^m(\cos \theta) e^{im\varphi}, \quad (\text{A1})$$

where $\hat{\mathbf{r}} = \mathbf{r}/r$, (r, θ, φ) are the spherical coordinates, and $P_j^m(\cos \theta)$ are the Legendre polynomials. The vector spherical harmonics are defined as

$$\mathbf{y}_{jm0} = [j(j+1)]^{-1/2} r \nabla_{\Omega} Y_{jm},$$

$$\mathbf{y}_{jm1} = -i \hat{\mathbf{r}} \times \mathbf{y}_{jm0}, \quad (\text{A2})$$

$$\mathbf{y}_{jm2} = \hat{\mathbf{r}} Y_{jm},$$

where ∇_{Ω} denotes the angular part of the gradient operator. \mathbf{y}_{jm0} and \mathbf{y}_{jm1} are tangential, while \mathbf{y}_{jm2} is normal to a sphere.

Divergence of the product of \mathbf{y}_{jmq} and arbitrary function of $r, h(r)$ is

$$\nabla \cdot [h(r) \mathbf{y}_{jm0}] = -[j(j+1)]^{1/2} \frac{h(r)}{r} Y_{jm},$$

$$\nabla \cdot [h(r) \mathbf{y}_{jm1}] = 0, \quad (\text{A3})$$

$$\nabla \cdot [h(r) \mathbf{y}_{jm2}] = \left(\frac{d}{dr} + \frac{2}{r} \right) h(r) Y_{jm}.$$

2. Recoupling the products of spherical harmonics

The product of scalar harmonics is recoupled as

$$Y_{jm} Y_{j_1 m_1} = \sum_{j_2 m_2} 2 \zeta(j, j_1, j_2, m, m_1, m_2, 2) Y_{j_2 m_2}. \quad (\text{A4})$$

The vector-harmonic expansion of a product of vector and scalar harmonics has the form

$$\mathbf{y}_{jmq} Y_{j_1 m_1} = \sum_{j_2 m_2 q_2} \mathbf{C}_{qq_2}(j, j_1, j_2) \times \zeta(j, j_1, j_2, m, m_1, m_2, q + q_2) \mathbf{y}_{j_2 m_2 q_2}. \quad (\text{A5})$$

The nonzero elements of the coupling matrix $\mathbf{C}_{qq_2}(j, j_1, j_2)$,

$$C_{00} = C_{11} = [j(j+1)j_2(j_2+1)]^{1/2} \chi(j, j_1, j_2),$$

$$C_{01} = C_{10} = -[j(j+1)j_2(j_2+1)]^{1/2} \theta(j, j_1, j_2), \quad (\text{A6})$$

$$C_{22} = 2.$$

Since tangential ($q=0, 1$) and radial $q=2$ harmonics are orthogonal,

$$C_{q2} = 0 \quad \text{and} \quad C_{2q} = 0, \quad q = 0, 1. \quad (\text{A7})$$

The scalar-harmonic expansion of the product of two vector harmonics has the form

$$\mathbf{y}_{jmq} \cdot \mathbf{y}_{j_1 m_1 q_1} = \sum_{j_2 m_2} \mathbf{C}_{qq_1}(j, j_2, j_1) (-1)^{\delta_{q2} \delta_{q_1 2}} \times \zeta(j, j_1, j_2, m, m_1, m_2, q + q_1) Y_{j_2 m_2}. \quad (\text{A8})$$

In these equations

$$\chi(j, j_1, j_2) = j(j+1) + j_2(j_2+1) - j_1(j_1+1), \quad (\text{A9})$$

$$\theta(j, j_1, j_2) = [(j + j_1 - j_2)(j - j_1 + j_2)(1 - j + j_1 + j_2) \times (1 + j + j_1 + j_2)]^{1/2}, \quad (\text{A10})$$

and the Clebsch-Gordan coefficient is

$$\begin{aligned} & \zeta(j, j_1, j_2, m, m_1, m_2, q + q_2) \\ &= \frac{(-1)^{m_2}}{2} \left(\frac{(2j+1)(2j_1+1)(2j_2+1)}{4\pi} \right)^{1/2} \\ & \times \begin{pmatrix} j - \xi & j_1 & j_2 \\ 0 & 0 & 0 \end{pmatrix} \begin{pmatrix} j & j_1 & j_2 \\ m & m_1 & -m_2 \end{pmatrix}, \end{aligned} \quad (\text{A11})$$

where $\xi=1$ if $q+q_2$ is even (or zero) and $\xi=0$ if $q+q_2$ is odd.

$$\begin{pmatrix} j & j_1 & j_2 \\ m & m_1 & m_2 \end{pmatrix}$$

is the Wigner $3j$ symbol.⁴⁴ The $3j$ symbol vanishes,

$$\begin{pmatrix} j & j_1 & j_2 \\ m & m_1 & m_2 \end{pmatrix} = 0, \quad (\text{A12})$$

unless

$$m + m_1 + m_2 = 0, \quad (\text{A13})$$

and the triangular condition

$$-j + j_1 + j_2 \geq 0,$$

$$j - j_1 + j_2 \geq 0, \quad (\text{A14})$$

$$j + j_1 - j_2 \geq 0$$

is satisfied. Also,

$$\begin{pmatrix} j & j_1 & j_2 \\ 0 & 0 & 0 \end{pmatrix} = 0, \quad (\text{A15})$$

unless

$$j + j_1 + j_2 = 2k, \quad k = 1, 2, \dots \quad (\text{A16})$$

3. Spherical tensors basis

The orthonormal traceless tensors \mathbf{a}_{jm} are defined by the relation²⁸

$$\hat{\mathbf{r}} \cdot \mathbf{a}_{jm} = \left(\frac{j+1}{2j+1} \right)^{1/2} \mathbf{y}_{jm0} + \left(\frac{j}{2j+1} \right)^{1/2} \mathbf{y}_{jm2}. \quad (\text{A17})$$

The explicit expressions for the complete set are

$$\mathbf{a}_{20} = \frac{1}{\sqrt{6}} \begin{pmatrix} -1 & 0 & 0 \\ 0 & -1 & 0 \\ 0 & 0 & 2 \end{pmatrix}, \quad (\text{A18a})$$

$$\mathbf{a}_{2\pm 1} = \begin{pmatrix} 0 & 0 & \mp \frac{1}{2} \\ 0 & 0 & -\frac{i}{2} \\ \mp \frac{1}{2} & -\frac{i}{2} & 0 \end{pmatrix}, \quad (\text{A18b})$$

$$\mathbf{a}_{2\pm 2} = \begin{pmatrix} \frac{1}{2} & \pm \frac{i}{2} & 0 \\ \pm \frac{i}{2} & -\frac{1}{2} & 0 \\ 0 & 0 & 0 \end{pmatrix}. \quad (\text{A18c})$$

4. Fundamental set of velocity fields

Following the definitions given in Ref. 28, we list the expressions for the functions $\mathbf{V}_{jmq}^{\pm}(\Omega)$ that characterize the angular dependence of the velocity fields (48) and (49):

$$\mathbf{V}_{jm0}^{-} = \frac{(2-j)}{2(4j^2-1)} \left[\left(\frac{j+1}{j} \right)^{1/2} \mathbf{y}_{jm0} + \frac{(j+1)}{(2-j)} \mathbf{y}_{jm2} \right], \quad (\text{A19a})$$

$$\mathbf{V}_{jm1}^{-} = (2j+1)^{-1} [j(j+1)]^{-1/2} \mathbf{y}_{jm1}, \quad (\text{A19b})$$

$$\mathbf{V}_{jm2}^{-} = \frac{j}{(2j+1)^2(2j+3)} \left[\left(\frac{j}{j+1} \right)^{1/2} \mathbf{y}_{jm0} - \mathbf{y}_{jm2} \right], \quad (\text{A19c})$$

$$\mathbf{V}_{jm0}^{+} = \left(\frac{j+1}{j} \right)^{1/2} \left(j \mathbf{y}_{jm0} + \frac{1}{2}(j+3)(2j+1) \mathbf{y}_{jm2} \right), \quad (\text{A20a})$$

$$\mathbf{V}_{jm1}^{+} = [j(j+1)]^{1/2} \mathbf{y}_{jm1}, \quad (\text{A20b})$$

$$\mathbf{V}_{jm2}^{+} = j \mathbf{y}_{jm0} + \frac{1}{2}(j+1)(2j+1) \mathbf{y}_{jm2}. \quad (\text{A20c})$$

APPENDIX B: EXPANSIONS OF GEOMETRIC QUANTITIES

Evaluation of the interfacial stresses involves geometric quantities such as the normal vector (23) and the curvature

$$K_H = \nabla \cdot \mathbf{n}. \quad (\text{B1})$$

These are expanded in the small parameter ε as

$$\mathbf{n}(\Omega) = \hat{\mathbf{r}} + \sum_{p=1}^{\infty} \varepsilon^p \mathbf{n}_p(\Omega), \quad (\text{B2})$$

$$K_H(\Omega) = 2 + \sum_{p=1}^{\infty} \varepsilon^p H_p(\Omega). \quad (\text{B3})$$

1. Normal vector

The normal vector is expanded in vector spherical harmonics

$$\mathbf{n}_p = n_{jmq}^{(p)}(\mathbf{f}) \mathbf{y}_{jmq}. \quad (\text{B4})$$

Introducing the above expansion for the normal vector along with the expansion for the gradient of f (B12) into the normal vector definition (23) results in a complicated expansion. Here the first three expansion terms, which are needed for our calculation, are listed:

$$n_{jmq}^{(1)} = -\delta_{q0} f_{jm} [j(j+1)]^{1/2}, \quad (\text{B5})$$

$$n_{jm0}^{(2)} = \sum' f_{j_1 m_1} f_{j_2 m_2} \zeta(j_1, j_2, j, m_1, m_2, m, 0) \times [j(j+1)]^{-1/2} \chi(j_1, j_2, j),$$

$$n_{jm1}^{(2)} = 0, \quad (\text{B6})$$

$$n_{jm2}^{(2)} = \frac{1}{2} \sum' f_{j_1 m_1} f_{j_2 m_2} \zeta(j_1, j_2, j, m_1, m_2, m, 0) \chi(j_1, j, j_2).$$

The summation over the j indices is from 2 to j_{\max} ; for each j index m takes values from $-j$ to j , i.e.,

$$\sum' \equiv \sum_{j_1 m_1 j_2 m_2} = \sum_{j_1=2}^{j_{\max}} \sum_{m_1=-j_1}^{j_1} \sum_{j_2=2}^{j_{\max}} \sum_{m_2=-j_2}^{j_2}. \quad (\text{B7})$$

2. Curvature

The curvature (B3) is expanded in scalar spherical harmonics

$$H_p = H_{jm}^{(p)}(\mathbf{f}) Y_{jm}. \quad (\text{B8})$$

This expansion is obtained after inserting the expansion of the normal vector (B4) into the definition of the curvature (B1), recoupling the harmonics products according to (A5) and taking divergence of the result according to (A3). The first three expansion terms, which are needed for the calculation of interfacial stresses, are

$$H_{jm}^{(1)} = -2 + j(j+1) f_{jm}, \quad (\text{B9})$$

$$H_{jm}^{(2)} = \sum' f_{j_1 m_1} f_{j_2 m_2} \zeta(j_1, j_2, j, m_1, m_2, m, 0) \times 2[2 + j_1(j_1 + 1)], \quad (\text{B10})$$

where the summation Σ' is defined by (B7).

3. Gradient of shape perturbation

Using the spherical harmonic representation of f (33a), the definition of the vector spherical harmonic \mathbf{y}_{jm0} (A2), and Eq. (13), we obtain

$$\nabla f = f_{jm} [j(j+1)]^{1/2} \mathbf{y}_{jm0} r_s^{-1}. \quad (\text{B11})$$

Expanding in Taylor series around the spherical drop shape and recoupling the spherical harmonics products leads to

$$\nabla f = \sum_{n=0}^{\infty} \varepsilon^n (-1)^n N_{jmq}^{(n)}(\mathbf{f}) \mathbf{y}_{jmq}, \quad q = 0, 1. \quad (\text{B12})$$

Since the product of a tangential vector harmonic with a scalar harmonic (A5) generates only tangential harmonics, the expansion of (B11) contains only tangential harmonics. The general form of the expansion coefficients is

$$N_{jmq}^{(n)}(\mathbf{f}) = \sum' \Phi_{j_2 m_2}^{(n)}(\mathbf{f}) f_{j_1 m_1} [j_1(j_1 + 1)]^{1/2} \times C_{0q}(j_1, j_2, j) \zeta(j_1, j_2, j, m_1, m_2, m, q), \quad (\text{B13})$$

where $\Phi_{lm,n}$ is given by Eqs. (B16) and (B17). The explicit expressions for the first two terms in the expansion are

$$N_{jmq}^{(0)} = \delta_{q0} f_{jm} [j(j+1)]^{1/2}, \quad (\text{B14a})$$

$$N_{jm0}^{(1)} = \sum' f_{j_1 m_1} f_{j_2 m_2} [j(j+1)]^{-1/2} \times \chi(j_1, j_2, j) \zeta(j_1, j_2, j, m_1, m_2, m, 0),$$

$$N_{jm1}^{(1)} = 0. \quad (\text{B14b})$$

4. Product of shape parameters

The product of k shape parameters f^k (or similarly surfactant parameters g) involves a product of k spherical harmonics:

$$f^k \equiv f_{j_1 m_1} Y_{j_1 m_1} f_{j_2 m_2} Y_{j_2 m_2} \cdots f_{j_k m_k} Y_{j_k m_k}. \quad (\text{B15})$$

After recoupling we obtain

$$f^k = \Phi_{lm_1}^{(k)}(\mathbf{f}) Y_{lm_1}. \quad (\text{B16})$$

The coefficient $\Phi_{lm_1}^{(k)}(\mathbf{f})$ is a homogeneous function of order k of \mathbf{f} . It is evaluated by the following recursive formula:

$$\Phi_{jm}^{(k)} = \sum_{j_1=0}^{(k-1)j_{\max}} \sum_{m_1=-j_1}^{j_1} \Phi_{j_1 m_1}^{(k-1)} \sum_{j_2=2}^{j_{\max}} \sum_{m_2=-j_2}^{j_2} f_{j_2 m_2} \times \zeta(j_1, j_2, j, m_1, m_2, m, 4) C_{22}(j_1, j_2, j), \quad (\text{B17})$$

where

$$\Phi_{jm}^{(2)} = \sum_{j_1=2}^{j_{\max}} \sum_{j_2=2}^{j_{\max}} \sum_{m_1=-j_1}^{j_1} \sum_{m_2=-j_2}^{j_2} f_{j_1 m_1} f_{j_2 m_2} \times \zeta(j_1, j_2, j, m_1, m_2, m, 4) C_{22}(j_1, j_2, j). \quad (\text{B18})$$

APPENDIX C: INTERFACIAL STRESSES

Since hydrostatic pressure does not affect the hydrodynamics, we exclude the isotropic normal interfacial stresses

$$\hat{\mathbf{t}} = \mathbf{t} - \mathbf{n} \langle \mathbf{t} \cdot \mathbf{n} \rangle_{\Omega}, \quad (\text{C1})$$

where the angular average of a quantity b is defined as

$$\langle b \rangle_{\Omega} \equiv \frac{1}{4\pi} \int b \, d\Omega. \quad (\text{C2})$$

The leading order term in the interfacial stresses expansion (54) corresponds to a spherical drop with uniform surfactant coverage. Since the isotropic part is subtracted, according to (6), we have

$$\hat{\mathbf{t}}_{jmq}^{(0)} = 0. \quad (\text{C3})$$

In this appendix we list only the expression for the expansion terms of first and second perturbation order; the third-order formulas are very cumbersome; these are available from the authors upon request.

1. Capillary stress

Substituting the expansions for the normal vector (B4) and curvature (B8) into the definition of interfacial stress (11) and recoupling the harmonics products yields the expansion for the capillary stresses in Eq. (58). This procedure yields for the first-order term

$$t_{jm}^{(1),cap} = \delta_{q2} \{-2 + [j(j+1)]\} f_{jm}. \tag{C4}$$

The general form for the second-order term is

$$t_{jm}^{(2),cap} = \sum' f_{j_1 m_1} f_{j_2 m_2} \zeta(j_1, j_2, j, m_1, m_2, m, q) \times \bar{t}_{jm}^{(2),cap}(j, j_1, j_2), \tag{C5}$$

where

$$\begin{aligned} \bar{t}_{jm}^{(2),cap} &= [j(j+1)]^{-1/2} (2 - j_2 - j_2^2) \chi(j_1, j_2, j), \\ \bar{t}_{jm}^{(2),cap} &= [j(j+1)]^{-1/2} (j_2 + j_2^2) \theta(j_1, j_2, j), \\ \bar{t}_{jm}^{(2),cap} &= 4(1 - j_2 - j_2^2). \end{aligned} \tag{C6}$$

2. Marangoni stress

Marangoni stresses (12) are more complicated to recast into expansion of vector spherical harmonics because they involve expanding and recoupling the product of normal vector, curvature, and surfactant concentration.

Marangoni stresses consist of a normal part, proportional to curvature, and tangential part, which includes the surface gradients of surfactant concentration

$$t^{mar} = t_n^{mar} + t_t^{mar}, \tag{C7}$$

where

$$\begin{aligned} t_n^{mar} &= -(\Gamma H - \langle \Gamma H \rangle_\Omega) \mathbf{n}, \\ t_t^{mar} &= (\mathbf{I} - \mathbf{nn}) \cdot \nabla \Gamma. \end{aligned} \tag{C8}$$

Let the definition of the angular surfactant concentration (26) be rewritten as

$$\Gamma(\mathbf{r}) = \Gamma_\Omega(\Omega) h(r, \Omega), \tag{C9}$$

where

$$h(r, \Omega) = \frac{\hat{\mathbf{r}} \cdot \mathbf{n}}{r^2} \tag{C10}$$

is in fact the inverse of the Jacobian (27). In this notation, taking the gradient of the above equation results in

$$\nabla \Gamma = \Gamma_\Omega \frac{dh(r, \Omega)}{dr} + \frac{1}{r} \nabla_\Omega [\Gamma_\Omega(\Omega) h(r, \Omega)]. \tag{C11}$$

After lengthy algebra, performed by MATHEMATICA, which involves expanding and recoupling of harmonics products, we obtain for the first-order Marangoni stress expansion term

$$\begin{aligned} \bar{t}_{jm}^{(1),mar} &= -\{2g_{jm} + [-6 + j(j+1)]f_{jm}\}, \\ \bar{t}_{jm}^{(1),mar} &= 0, \end{aligned} \tag{C12}$$

$$\bar{t}_{jm}^{(1),mar} = [j(j+1)]^{1/2} (g_{jm} - 2f_{jm}).$$

The general form for the second-order term is

$$t_{jm}^{(2),mar} = \sum' \zeta(j_1, j_2, j, m_1, m_2, m, q) \bar{t}_{jm}^{(2),mar}(j, j_1, j_2), \tag{C13}$$

where

$$\begin{aligned} \bar{t}_{jm}^{(2),mar} &= f_{j_2 m_2} \{[-24 + 6j_2(j_2 + 1) + \chi(j_2, j_1, j)] f_{j_1 m_1} \\ &\quad - [-12 + \chi(j_2, j_1, j)] g_{j_1 m_1}\}, \\ \bar{t}_{jm}^{(2),mar} &= f_{j_2 m_2} [j(j+1)]^{-1/2} \theta(j_1, j_2, j) \\ &\quad \times [- (j_2 + j_2^2) f_{j_1 m_1} + 3g_{j_1 m_1}], \\ \bar{t}_{jm}^{(2),mar} &= f_{j_2 m_2} [j(j+1)]^{-1/2} \\ &\quad \times \left\{ \left[-\frac{1}{2} (j + j^2) \chi(j_1, j, j_2) + (2 + j_2 + j_2^2) \chi(j_1, j_2, j) \right] \right. \\ &\quad \left. \times f_{j_1 m_1} - 3\chi(j_1, j_2, j) g_{j_1 m_1} \right\}. \end{aligned} \tag{C14}$$

and the summation is defined according to Eq. (B7).

APPENDIX D: DROP SHAPE AND SURFACTANT DISTRIBUTION EVOLUTION COEFFICIENTS

To avoid lengthy expressions, here we list the expansion terms for the rescaled evolution equations (61) and (62). Using the rules from Appendix F these are easily transformed into the expansion for the actual quantities.

The leading order term in the evolution equations describes the distortion of drop shape and surfactant distribution by the extensional component of the flow:

$$S_{jm}^{F,(0)} = \beta_{2m} \delta_{j2} 4 \sqrt{\frac{\pi}{30}}, \tag{D1}$$

$$S_{jm}^{\Gamma,(0)} = \beta_{2m} \delta_{j2} 2 \sqrt{\frac{6\pi}{5}}.$$

The rotational component of the flow, if present, tends to misalign the deformed shape and surfactant distribution away from the extensional axes of the flow, thus producing an effectively restoring effect that appears at the next order:

$$S_{jm}^{F,(1)} = i\omega \frac{m}{2} f_{jm}, \tag{D2}$$

$$S_{jm}^{\Gamma,(1)} = i\omega \frac{m}{2} g_{jm}.$$

The axisymmetric extensional flow $\mathbf{u}^\infty = (-\frac{1}{2}x, -\frac{1}{2}y, z)$ is given by $\beta_{2m} = \delta_{m0} (1/2\sqrt{6})$ and no rotational part, $\omega = 0$; hence, $m = 0$ always. Simple shear flow $\mathbf{u}^\infty = (y, 0, 0)$ is given by $\beta_{2m} = (i/2)\text{sign}(m)\delta_{|m|2}$ and $\omega = 1$. These are the only non-

zero contributions generated by the imposed flow. The rest of the perturbation expansion terms correspond to the interfacial stress-driven relaxation. The first-order terms are

$$K_{jm}^{\nu,(1)} = \bar{K}_{jm,1}^{\nu}(j)f_{jm}, \quad \nu = F, \Gamma, \quad (\text{D3})$$

$$M_{jm}^{\nu,(1)} = \bar{M}_{jm,f}^{\nu}(j)f_{jm} + \bar{M}_{jm,g}^{\nu}(j)g_{jm},$$

where the shape evolution coefficients are

$$\begin{aligned} \bar{K}_{jm,1}^F &= 2d(j)j(1-j^2)(j+2), \\ \bar{M}_{jm,f}^F &= 2d(j)j(j+1)(-3+j(j+1)), \end{aligned} \quad (\text{D4})$$

$$\bar{M}_{jm,g}^F = d(j)j(j+1),$$

and for the surfactant evolution coefficients are

$$\begin{aligned} \bar{K}_{jm,1}^{\Gamma} &= 3d(j)j(1-j^2)(j+2), \\ \bar{M}_{jm,f}^{\Gamma} &= -d(j)j(j+1)(12-7j(j+1)), \end{aligned} \quad (\text{D5})$$

$$\bar{M}_{jm,g}^{\Gamma} = -d(j)j(j+1)(-3+2j(j+1)),$$

and

$$d(j) = [(2j+1)(2j-1)(2j+3)]^{-1}. \quad (\text{D6})$$

The second-order terms have the general form

$$\begin{aligned} A_{jm}^{(2)} &= \sum' \zeta(j_1, j_2, j, m_1, m_2, m) [\bar{A}_1(j_1, j_2, j) f_{j_1 m_1} f_{j_2 m_2} \\ &\quad + \bar{A}_2(j_1, j_2, j) f_{j_1 m_1} g_{j_2 m_2} + \bar{A}_3(j_1, j_2, j) g_{j_1 m_1} f_{j_2 m_2} \\ &\quad + \bar{A}_4(j_1, j_2, j) g_{j_1 m_1} g_{j_2 m_2}], \end{aligned} \quad (\text{D7})$$

where A stands for $K^F, M^F, K^{\Gamma}, M^{\Gamma}$ and the summation Σ' is defined by (B7):

$$\begin{aligned} \bar{K}_1^F &= d(j_1)(-2+j_1+j_1^2)[3\chi(j_1, j, j_2) + 2j_1(j_1+1)] \\ &\quad + d(j)[3(-2+j_2+j_2^2)\chi(j_1, j_2, j) \\ &\quad + 2(j+j^2)(-2+j_1+j_1^2)], \end{aligned} \quad (\text{D8})$$

$$\bar{K}_i^F = 0, \quad i = 2, 3, 4,$$

$$\begin{aligned} \bar{K}_1^{\Gamma} &= d(j)\{12(j+j^2)(j_1+j_1^2-1) - (3+2j+2j^2) \\ &\quad \times [2j^2(j^2+1)^2 - \chi(j_2, j_1, j)(2+2j+2j^2-j_2-j_2^2)]\} \\ &\quad + d(j_1)(-2+j_1+j_1^2)(3+2j_1+2j_1^2)\chi(j_1, j_2, j), \end{aligned}$$

$$\bar{K}_2^{\Gamma} = 3d(j_1)(2-j_1-j_1^2)\chi(j_1, j_2, j), \quad (\text{D9})$$

$$\bar{K}_i^{\Gamma} = 0, \quad i = 3, 4,$$

$$\begin{aligned} \bar{M}_1^F &= -\frac{3}{2}d(j)[2j(j+1)[-2+3\chi(j_1, 1, j)] - \chi(j_2, j_1, j)(-4 \\ &\quad + j+j^2+2j_2+2j_2^2)] \\ &\quad + d(j_1)[\chi(j_1, j, j_2)(12-7j_1-7j_1^2) + 6(j_1+j_1^2)^2], \end{aligned}$$

$$\bar{M}_2^F = 2d(j)(j+j^2)[\chi(j_1, j_2, j) - 12],$$

$$\begin{aligned} \bar{M}_3^F &= d(j_1)[\chi(j_1, j_2, j)(3-2j_1-2j_1^2) - 4j_1-4j_1^2] + d(j) \\ &\quad \times [12j+12j^2 + \chi(j_1, j_2, j)(3+2j+2j^2)], \\ \bar{M}_4^F &= 0, \end{aligned} \quad (\text{D10})$$

$$\begin{aligned} \bar{M}_1^{\Gamma} &= \frac{1}{2}d(j)c_1 - d(j_1)\chi(j_1, j_2, j) \\ &\quad \times (-12-5j_1+11j_1^2+12j_1^3+2j_1^4), \end{aligned} \quad (\text{D11a})$$

where

$$\begin{aligned} c_1 &= 10j^5 - 2j^6 + 4j^3(-22+9j_1+9j_1^2-5j_2-5j_2^2) \\ &\quad + j^4(-19+10j_1+10j_1^2-2j_2-2j_2^2) - 6j_2(1+j_2) \\ &\quad \times [j_1+j_1^2-j_2(1+j_2)] + j^2[15-27j_2-23j_2^2+8j_2^3+4j_2^4 \\ &\quad + (j_1+j_1^2)(11-4j_2-4j_2^2)] + j[72+3j_2+7j_2^2+8j_2^3 \\ &\quad + 4j_2^4 - (j_1+j_1^2)(27+4j_2+4j_2^2)], \end{aligned} \quad (\text{D11b})$$

$$\begin{aligned} \bar{M}_2^{\Gamma} &= d(j_1)(-12+7j_1+7j_1^2)\chi(j_1, j_2, j) \\ &\quad + 3d(j)j(j+1)[-12+\chi(j_1, j_2, j)], \end{aligned} \quad (\text{D12})$$

$$\bar{M}_3^{\Gamma} = d(j_1)(1+j_1^2)(-3+4j_1)\chi(j_1, j_2, j) + d(j_1)c_3, \quad (\text{D13a})$$

where

$$\begin{aligned} c_3 &= j^4 - 4j^5 + 2j(9+2j_1+2j_1^2-2j_2-2j_2^2) - 3j^2(-10 \\ &\quad + j_1+j_1^2-j_2-j_2^2) + j^3(17-4j_1-4j_1^2+4j_2+4j_2^2) \\ &\quad + 6[j_1+j_1^2-j_2(1+j_2)], \end{aligned} \quad (\text{D13b})$$

$$\bar{M}_4^{\Gamma} = -d(j_1)(-3+2j_1+2j_1^2)\chi(j_1, j_2, j). \quad (\text{D14})$$

Expressions for the third-order terms become rather cumbersome. These are available upon request from the authors.

APPENDIX E: VELOCITY FIELDS

Disturbance flow field is generated only by the interfacial stresses, which “switch on” only after deformation is inflicted by the incident flow. Therefore, at the leading order there is no disturbance velocity field (47), and

$$c_{jmq}^{(0)} = 0. \quad (\text{E1})$$

The first-order perturbation solution for the velocity field is

$$\begin{aligned} c_{jmq}^{(1)} &= \kappa f_{jm} \bar{C}_{jmq,1} + \text{Ma} f_{jm} \bar{C}_{jmq,2} + \text{Ma} g_{jm} \bar{C}_{jmq,3}, \\ q &= 0, 2, \end{aligned} \quad (\text{E2})$$

$$c_{jm1}^{(1)} = 0,$$

where

$$\begin{aligned} \bar{C}_{jm0,1} &= \frac{1}{2}(j^2-1)(j+2)(2j+1), \\ \bar{C}_{jm2,1} &= j(j-1)(j+2), \end{aligned} \quad (\text{E3a})$$

$$\bar{C}_{jm0,2} = -\frac{1}{2}j(j+1)(j+3)(2j+1), \quad \hat{C}_{jm1,3} = 0, \quad (\text{E5i})$$

$$\bar{C}_{jm2,2} = -j(j-1)(j+4), \quad (\text{E3b}) \quad \hat{C}_{jm0,4} = -6j - 5j^2 + j^3 - 2j_1 + jj_1 - 2j_1^2 + jj_1^2 + 2j_2 - jj_2 + 2j_2^2 - jj_2^2, \quad (\text{E5j})$$

$$\bar{C}_{jm0,3} = -\frac{1}{2}(j+1)^2(2j+1), \quad \hat{C}_{jm1,4} = \frac{1}{2}(3+7j+2j^2)(-4-3j+j^2+j_1+j_1^2-j_2-j_2^2), \quad (\text{E5k})$$

$$\bar{C}_{jm2,3} = -j(j-1). \quad (\text{E3c})$$

The second-order velocity fields are

$$c_{jm}^{(2)} = \sum' \zeta(j_1, j_2, j, m_1, m_2, m) \times (\kappa f_{j_1 m_1} f_{j_2 m_2} \hat{C}_{jm} + \text{Ma} f_{j_1 m_1} f_{j_2 m_2} \hat{C}_{jm,2} + \text{Ma} f_{j_1 m_1} g_{j_2 m_2} \hat{C}_{jm,3} + \text{Ma} g_{j_1 m_1} f_{j_2 m_2} \hat{C}_{jm,4}), \quad (\text{E4})$$

where the summation is according to Eq. (B7), $\zeta(j_1, j_2, j, m_1, m_2, m)$ is defined by (A11), and

$$\hat{C}_{jm0,1} = 2j - 2j^2 + 2j_1 - 2jj_1 + 2j_1^2 j_1 + 2j_1^2 - 2j_1^2 j_1^2 + 2j_1^2 j_1^2 - 2j_2 - jj_2 - j^2 j_2 - j_1 j_2 - j_1^2 j_2 - j_2^2 - jj_2^2 - j^2 j_2^2 - j_1 j_2^2 - j_1^2 j_2^2 + 2j_2^3 + j_2^4, \quad (\text{E5a})$$

$$\hat{C}_{jm2,1} = \frac{2j+1}{2j} (-2j - 4j^2 - 2j^3 + 6j_1 + 4jj_1 + 4j^2 j_1 + 2j_1^3 j_1 + 6j_1^2 + 4jj_1^2 + 4j^2 j_1^2 + 2j_1^3 j_1^2 - 6j_2 - 5jj_2 - 4j^2 j_2 - j^3 j_2 - 3j_1 j_2 - jj_1 j_2 - 3j_1^2 j_2 - jj_1^2 j_2 - 3j_2^2 - 4jj_2^2 - 4j^2 j_2^2 - j^3 j_2^2 - 3j_1 j_2^2 - jj_1 j_2^2 - 3j_1^2 j_2^2 - jj_1^2 j_2^2 + 6j_2^3 + 2jj_2^3 + 3j_2^4 + jj_2^4), \quad (\text{E5b})$$

$$\hat{C}_{jm1,1} = (j_2 + j_2^2)(j + j^2)^{1/2}, \quad (\text{E5c})$$

$$\hat{C}_{jm0,2} = \frac{2j+1}{4j} (9j^2 + 11j^3 + 3j^4 + j^5 - 24j_1 - 21jj_1 - 10j^2 j_1 - 5j^3 j_1 - 24j_1^2 - 21jj_1^2 - 10j^2 j_1^2 - 5j^3 j_1^2 + 24j_2 + 21jj_2 + 6j^2 j_2 + j^3 j_2 + 6j_1 j_2 + 2jj_1 j_2 + 6j_1^2 j_2 + 2jj_1^2 j_2 + 18j_2^2 + 19jj_2^2 + 6j^2 j_2^2 + j^3 j_2^2 + 6j_1 j_2^2 + 2jj_1 j_2^2 + 6j_1^2 j_2^2 + 2jj_1^2 j_2^2 - 12j_2^3 - 4jj_2^3 - 6j_2^4 - 2jj_2^4), \quad (\text{E5d})$$

$$\hat{C}_{jm2,2} = \frac{1}{2} (-24j + 23j^2 + j^4 + 5jj_1 - 5j^2 j_1 + 5jj_1^2 - 5j^2 j_1^2 + 3jj_2 + j^2 j_2 + 2j_1 j_2 + 2j_1^2 j_2 - 2j_2^2 + 3jj_2^2 + j^2 j_2^2 + 2j_1 j_2^2 + 2j_1^2 j_2^2 - 4j_2^3 - 2j_2^4), \quad (\text{E5e})$$

$$\hat{C}_{jm1,2} = (4 + 2j - j_2 - j_2^2)(j + j^2)^{1/2}, \quad (\text{E5f})$$

$$\hat{C}_{jm0,3} = -j(-12 + j + j^2 + j_1 + j_1^2 - j_2 - j_2^2), \quad (\text{E5g})$$

$$\hat{C}_{jm2,3} = -\frac{1}{2}(1 + 3j + 2j^2)(-12 + j + j^2 + j_1 + j_1^2 - j_2 - j_2^2), \quad (\text{E5h})$$

APPENDIX F: TRANSFORMATION FROM RESCALED TO ACTUAL QUANTITIES

Herein, we revert to using \sim for the rescaled variables. Substituting (16) and (17) into (61) and (62), which describe the evolution of the rescaled variables \tilde{f} and \tilde{g} , and noting that $\tilde{g} \equiv g$ leads to

$$F_{jm}^{(p)} = \alpha S_{jm}^{F,(p)} \left(\frac{\mathbf{f}}{\alpha}, \mathbf{g} \right) + \frac{\kappa}{\alpha} K_{jm}^{F,(p)} \left(\frac{\mathbf{f}}{\alpha}, \mathbf{g} \right) + \frac{\text{Ma}}{\alpha^2} M_{jm}^{F,(p)} \left(\frac{\mathbf{f}}{\alpha}, \mathbf{g} \right), \quad (\text{F1})$$

$$G_{jm}^{(p)} = S_{jm}^{\Gamma,(p)} \left(\frac{\mathbf{f}}{\alpha}, \mathbf{g} \right) + \frac{\kappa}{\alpha^2} K_{jm}^{\Gamma,(p)} \left(\frac{\mathbf{f}}{\alpha}, \mathbf{g} \right) + \frac{\text{Ma}}{\alpha^3} M_{jm}^{\Gamma,(p)} \left(\frac{\mathbf{f}}{\alpha}, \mathbf{g} \right).$$

In the above equations, the distinction between evolution terms describing flow-induced distortion, S , capillary relaxation, K , and Marangoni stress-driven relaxation, M , is explicitly made. The volume correction α , calculated from (15), is given by

$$\alpha = -\frac{s_2}{2\pi S} + \frac{Q}{2}, \quad (\text{F2})$$

where

$$Q^3 = 4 - \frac{s_3}{\pi} + \left[\left(\frac{s_2}{\pi} \right)^3 + \left(\frac{s_3}{\pi} - 4 \right)^2 \right]^{1/2}, \quad (\text{F3})$$

$$s_2 = \varepsilon^2 \sum_{l=2}^{j_{\max}} \sum_{m=-l}^l f_{lm} f_{l-m}, \quad (\text{F4})$$

and

$$s_3 = \varepsilon^3 2\sqrt{\pi} \Phi_{00,3}(\mathbf{f}). \quad (\text{F5})$$

$\Phi_{00,3}$ is calculated from (B17). For small deformations, α can be expanded in the small parameter ε :

$$\alpha = 1 - \varepsilon^2 \frac{1}{4\pi} f_{lm} f_{l-m} + \dots \quad (\text{F6})$$

After the α -containing terms are expanded in series of the small parameter ε and terms of the same order of ε are combined, we obtain the unrescaled evolution equations for the actual perturbations in shape and angular surfactant distribution identical in form with Eqs. (61) and (62).

The evolution coefficients in the rescaled evolution equations and the regular ones are simply related. These re-

lations for up to perturbation order 3 are (if not listed below the coefficients in rescaled and unrescaled expansions are the same)

$$S_{jm}^{F,(2)} = \tilde{S}_{jm}^{F,(2)} - \frac{\Delta}{4\pi} f_{j_1 m_1} f_{j_1 - m_1} \tilde{S}_{2m}^{F,(0)}, \quad (\text{F7})$$

$$K_{jm}^{F,(3)} = \tilde{K}_{jm}^{F,(3)} + \frac{\Delta}{4\pi} f_{j_1 m_1} f_{j_1 - m_1} f_{jm} \tilde{K}_{jm,1}^F,$$

$$M_{jm}^{F,(3)} = \tilde{M}_{jm}^{F,(3)} + \frac{3\Delta}{4\pi} f_{j_1 m_1} f_{j_1 - m_1} f_{jm} \tilde{M}_{jm,f}^F,$$

$$M_{jm}^{F,(3)} = \tilde{M}_{jm}^{F,(3)} + \frac{\Delta}{2\pi} f_{j_1 m_1} f_{j_1 - m_1} g_{jm} \tilde{M}_{jm,g}^F, \quad (\text{F8})$$

$$K_{jm}^{\Gamma,(3)} = \tilde{K}_{jm}^{\Gamma,(3)} + \frac{\Delta}{2\pi} f_{j_1 m_1} f_{j_1 - m_1} f_{jm} \tilde{K}_{jm,1}^{\Gamma},$$

$$M_{jm}^{\Gamma,(3)} = \tilde{M}_{jm}^{\Gamma,(3)} + \frac{\Delta}{\pi} f_{j_1 m_1} f_{j_1 - m_1} f_{jm} \tilde{M}_{jm,f}^{\Gamma},$$

$$M_{jm}^{\Gamma,(3)} = \tilde{M}_{jm}^{\Gamma,(3)} + \frac{3\Delta}{4\pi} f_{j_1 m_1} f_{j_1 - m_1} g_{jm} \tilde{M}_{jm,g}^{\Gamma}, \quad (\text{F9})$$

where

$$\Delta = \delta_{j_3 j} \delta_{j_1 j_2} \delta_{m_1 + m_2, 0} \delta_{m_3 m_2}, \quad (\text{F10})$$

and the rescaled evolutions coefficients are listed in Sec. IV.

- ¹F. Lequeux, "Emulsion rheology," *Curr. Opin. Colloid Interface Sci.* **3**, 408 (1998).
²C. Tucker and P. Moldenaers, "Microstructural evolution in polymer blends," *Annu. Rev. Fluid Mech.* **34**, 177 (2002).
³P. Van Puyvelde, S. Velankar, and P. Moldenaers, "Rheology and morphology of compatibilized polymer blend," *Curr. Opin. Colloid Interface Sci.* **6**, 457 (2001).
⁴H. A. Stone and L. G. Leal, "The effects of surfactants on drop deformation and breakup," *J. Fluid Mech.* **220**, 161 (1990).
⁵A. Williams, J. J. M. Janssen, and A. Prins, "Behaviour of droplets in simple shear flow in the presence of a protein emulsifier," *Colloids Surf., A* **125**, 189 (1997).
⁶Y. T. Hu, D. J. Pine, and L. G. Leal, "Drop deformation, breakup, and coalescence with compatibilizer," *Phys. Fluids* **12**, 484 (2000).
⁷S. Velankar, P. Van Puyvelde, J. Mewis, and P. Moldenaers, "Effect of compatibilization on the breakup of polymeric drops in shear flow," *J. Rheol.* **45**, 1007 (2001).
⁸S. Lyu, T. D. Jones, F. Bates, and C. W. Macosko, "Role of block copolymers on suppression of droplet coalescence," *Macromolecules* **35**, 7845 (2002).
⁹H. K. Jeon and C. W. Macosko, "Visualization of block copolymer distribution on a sheared drop," *Polymer* **44**, 5381 (2003).
¹⁰Y. Hu and A. Lips, "Estimating surfactant surface coverage and decomposing its effect on drop deformation," *Phys. Rev. Lett.* **91**, 044501 (2003).
¹¹S. Velankar, P. Van Puyvelde, J. Mewis, and P. Moldenaers, "Steady shear rheological properties of model compatibilized blends," *J. Rheol.* **48**, 725 (2004).
¹²M. R. Kennedy, C. Pozrikidis, and R. Skalak, "Motion and deformation of liquid drops and the rheology of dilute emulsions in simple shear flow," *Comput. Fluids* **23**, 251 (1994).
¹³M. Loewenberg and E. J. Hinch, "Numerical simulations of a concentrated emulsion in shear flow," *J. Fluid Mech.* **321**, 395 (1996).
¹⁴R. Charles and C. Pozrikidis, "Significance of the dispersed-phase viscosity on the simple shear flow of suspensions of two-dimensional liquid drops," *J. Fluid Mech.* **365**, 205 (1998).

- ¹⁵W. J. Milliken, H. A. Stone, and L. G. Leal, "The effect of surfactant on transient motion of newtonian drops," *Phys. Fluids A* **5**, 69 (1993).
¹⁶Y. Pawar and K. J. Stebe, "Marangoni effects on drop deformation in an extensional flow: The role of surfactant physical chemistry. I. Insoluble surfactants," *Phys. Fluids* **8**, 1738 (1996).
¹⁷X. Li and C. Pozrikidis, "The effect of surfactants on drop deformation and on the rheology of dilute emulsions in Stokes flow," *J. Fluid Mech.* **341**, 165 (1997).
¹⁸S. Yon and C. Pozrikidis, "A finite-volume/boundary-element method for flow past interfaces in the presence of surfactants, with application to shear flow past a viscous drop," *Comput. Fluids* **27**, 879 (1998).
¹⁹C. D. Eggleton, Y. P. Pawar, and K. J. Stebe, "Insoluble surfactants on a drop in an extensional flow: A generalization of the stagnated surface limit to deforming interfaces," *J. Fluid Mech.* **385**, 79 (1998).
²⁰M. A. Rother and R. H. Davis, "Buoyancy driven coalescence of spherical drops covered with incompressible surfactant at arbitrary Peclet number," *J. Colloid Interface Sci.* **270**, 205 (2004).
²¹C. Pozrikidis, "A finite-element method for interfacial surfactant transport, with application to the flow-induced deformation of a viscous drop," *J. Eng. Math.* **49**, 163 (2004).
²²J. M. Rallison, "The deformation of small viscous drops and bubbles in shear flows," *Annu. Rev. Fluid Mech.* **16**, 45 (1984).
²³H. A. Stone, "Dynamics of drop deformation and breakup in viscous fluids," *Annu. Rev. Fluid Mech.* **26**, 65 (1994).
²⁴R. G. Cox, "The deformation of a drop in a general time-dependent fluid flow," *J. Fluid Mech.* **37**, 601 (1969).
²⁵N. Frankel and A. Acrivos, "The constitutive equation for a dilute emulsion," *J. Fluid Mech.* **44**, 65 (1970).
²⁶D. Barthès-Biesel and A. Acrivos, "Deformation and burst of a liquid droplet freely suspended in a linear shear field," *J. Fluid Mech.* **61**, 1 (1973).
²⁷J. M. Rallison, "Note on the time-dependent deformation of a viscous drop which is almost spherical," *J. Fluid Mech.* **98**, 625 (1980).
²⁸J. Bławdziewicz, P. Vlahovska, and M. Loewenberg, "Rheology of a dilute emulsion of surfactant-covered spherical drops," *Physica A* **276**, 50 (2000).
²⁹P. Vlahovska, J. Bławdziewicz, and M. Loewenberg, "Nonlinear rheology of a dilute emulsion of surfactant-covered spherical drops in time-dependent flows," *J. Fluid Mech.* **463**, 1 (2002).
³⁰R. W. Flumerfelt, "Effects of dynamic interfacial properties on drop deformation and orientation in shear and extensional flow fields," *J. Colloid Interface Sci.* **76**, 330 (1980).
³¹S. Kim and S. J. Karrila, *Microhydrodynamics: Principles and Selected Applications* (Butterworth-Heinemann, London, 1991).
³²C. Pozrikidis, *Boundary Integral and Singularity Methods for Linearized Viscous Flow* (Cambridge University Press, Cambridge, 1992).
³³D. A. Edwards, H. Brenner, and D. T. Wasan, *Interfacial Transport Processes and Rheology* (Butterworth-Heinemann, Boston, 1991).
³⁴D. Barthès-Biesel, "Role of interfacial properties on the motion and deformation of capsules in shear flow," *Physica A* **172**, 103 (1991).
³⁵S. Dukhin, G. Kretschmar, and R. Miller, *Dynamics of Adsorption at Liquid Interfaces: Theory, Experiment, Application* (Elsevier, Amsterdam, 1995).
³⁶P. A. Kralchevsky, K. D. Danov, and I. B. Ivanov, "Thin liquid film physics," in *Foams. Theory, Measurements, and Applications*, edited by R. K. Prud'homme and S. A. Khan (Dekker, New York, 1996), pp. 1-98, see Table 2.
³⁷L. G. Leal, *Laminar Flow and Convective Transport Processes* (Butterworth-Heinemann, Boston, 1992).
³⁸H. A. Stone, "A simple derivation of the time-dependent convective-diffusion equation for surfactant transport along a deforming interface," *Phys. Fluids A* **2**, 111 (1990).
³⁹J. D. Jackson, *Classical Electrodynamics* (Wiley, New York, 1998).
⁴⁰B. Cichocki, B. U. Felderhof, and R. Schmitz, "Hydrodynamic interactions between two spherical particles," *PCH, PhysicoChem. Hydrodyn.* **10**, 383 (1988).
⁴¹P. Vlahovska, "Dynamics of a surfactant-covered drop and the non-Newtonian rheology of emulsions," Ph.D. thesis, Yale University, 2003, pdf file available by electronic mail: petia@aya.yale.edu
⁴²D. A. Varshalovich, A. N. Moskalev, and V. K. Khersonskii, *Quantum Theory of Angular Momentum* (World Scientific, Singapore, 1988).
⁴³M. N. Jones, *Spherical Harmonics and Tensors for Classical Field Theory* (Wiley, New York, 1985).
⁴⁴A. R. Edmonds, *Angular Momentum in Quantum Mechanics* (Princeton

- University Press, Princeton, 1960).
- ⁴⁵D. Barthès-Biesel and A. Acrivos, "Rheology of suspensions and its relation to phenomenological theories for non-Newtonian fluid," *Int. J. Multiphase Flow* **1**, 1 (1973).
- ⁴⁶V. Cristini, J. Bławdziewicz, and M. Loewenberg, "An adaptive mesh algorithm for evolving surfaces: Simulations of drop breakup and coalescence," *J. Comput. Phys.* **168**, 445 (2001).
- ⁴⁷A. Z. Zinchenko, M. A. Rother, and R. H. Davis, "A novel boundary-integral algorithm for viscous interaction of deformable drops," *Phys. Fluids* **9**, 1493 (1997).
- ⁴⁸G. I. Taylor, "The formation of emulsions in definable fields of flow," *Proc. R. Soc. London, Ser. A* **146**, 501 (1934).
- ⁴⁹Y. T. Hu and A. Lips, "Transient and steady state three-dimensional drop shapes and dimensions under planar extensional flow," *J. Rheol.* **47**, 349 (2003).
- ⁵⁰S. Guido and F. Greco, "Drop shape under slow steady shear flow and during relaxation. Experimental results and comparison with theory," *Rheol. Acta* **40**, 176 (2001).
- ⁵¹S. Guido and M. Villone, "Three-dimensional shape of a drop under simple shear flow," *J. Rheol.* **42**, 395 (1998).
- ⁵²R. D. Kamm, "Cellular fluid mechanics," *Annu. Rev. Fluid Mech.* **34**, 211 (2002).
- ⁵³U. Seifert, "Configurations of fluid membranes and vesicles," *Adv. Phys.* **46**, 13 (1997).
- ⁵⁴H. Dobreiner, "Properties of giant vesicles," *Curr. Opin. Colloid Interface Sci.* **5**, 256 (2000).
- ⁵⁵K. H. de Haas, C. Blom, D. van den Ende, M. H. G. Duits, and J. Mellema, "Deformation of giant lipid bilayer vesicles in shear flow," *Phys. Rev. E* **56**, 7132 (1997).
- ⁵⁶U. Seifert, "Fluid membranes in hydrodynamic flow fields: Formalism and an application to fluctuating quasispherical vesicles," *Eur. Phys. J. B* **8**, 405 (1999).
- ⁵⁷P. Olla, "The behavior of closed inextensible membranes in linear and quadratic shear flows," *Physica A* **278**, 87 (2000).